EXPERIMENTAL INVESTIGATION OF AN OIL LOSS MECHANISM IN INTERNAL COMBUSTION ENGINES

A THESIS SUBMITTED TO
THE GRADUATE SCHOOL OF NATURAL AND APPLIED SCIENCES
OF
MIDDLE EAST TECHNICAL UNIVERSITY

BY

AHMET SEZER

IN PARTIAL FULFILLMENT OF THE REQUIREMENTS FOR
THE DEGREE OF MASTER OF SCIENCE
IN
MECHANICAL ENGINEERING

MAY 2010

Approval of the thesis:

EXPERIMENTAL INVESTIGATION OF AN OIL LOSS MECHANISM IN INTERNAL COMBUSTION ENGINES

Submitted by **AHMET SEZER**, in partial fulfillment of the requirements for the degree of **Master of Science in Mechanical Engineering Department, Middle East Technical University** by,

Prof. Dr. Canan Özgen
Dean, **Graduate School of Natural and Applied Sciences** _____

Prof. Dr. Süha Oral
Head of Department, **Mechanical Engineering** _____

Prof. Dr. Zafer Dursunkaya
Supervisor, **Mechanical Engineering Dept., METU** _____

Examining Committee Members:

Prof. Dr. Kahraman Albayrak
Mechanical Engineering Dept., METU _____

Prof. Dr. Zafer Dursunkaya
Mechanical Engineering Dept., METU _____

Asst. Prof. Dr. Tuba Okutucu Özyurt
Mechanical Engineering Dept., METU _____

Asst. Prof. Dr. Ahmet Yozgatlıgil
Mechanical Engineering Dept., METU _____

Prof. Dr. İsmail H. Tuncer
Aerospace Engineering Dept., METU _____

I hereby declare that all information in this document has been obtained and presented in accordance with academic rules and ethical conduct. I also declare that, as required by these rules and conduct, I have fully cited and referenced all material and results that are not original to this work.

Ahmet SEZER

Signature :

ABSTRACT

EXPERIMENTAL INVESTIGATION OF AN OIL LOSS MECHANISM IN INTERNAL COMBUSTION ENGINES

Sezer, Ahmet
M.S., Department of Mechanical Engineering
Supervisor: Prof.Dr. Zafer DURSUNKAYA

May 2010, 90 pages

Oil loss mechanisms in internal combustion engines have been subject to many researches. By the help of technological developments effects of several problems due to oil losses were examined and tried to be reduced. Environmental pollution and performance loss are important issues that oil consumption in internal combustion engines contribute. In this study the effects of individual parameters on the oil accumulation in 2nd land crevice of internal combustion engines, volume between top compression rings, were investigated.

The study aimed to investigate the effects of oil film thickness and oil film temperature on the oil accumulation in the 2nd land which contributes to one of the mechanisms of oil consumption in internal combustion engines. Controlled experiments were performed on a modeled piston cylinder assembly.

It was seen that oil accumulated in the 2nd land crevice by blow-by gases was affected by the film thickness of lubricating oil and the temperature of the lubricating oil. The amount of oil accumulated increased with increasing oil film thickness. The

results also showed that below oil film thickness of 45 µm; amount of oil accumulated increased with the increase of oil temperature.

Keywords: Oil consumption, Oil accumulation, Oil film thickness, Oil film temperature, Oil blowback, Internal combustion engines.

ÖZ

İÇTEN YANMALI MOTORLARDA YAĞ KAYBI MEKANİZMASININ DENEYSEL İNCELENMESİ

Sezer, Ahmet
Yüksek Lisans, Makina Mühendisliği Bölümü
Tez Yöneticisi: Prof.Dr. Zafer DURSUNKAYA

Mayıs 2010, 90 sayfa

İçten yanmalı motorlarda yağ kaybı mekanizmaları birçok araştırmalara konu olmuştur. Gelişen teknolojiyle birlikte yağ kaybının nedenleri incelenmiş ve çözümler aranmıştır. İçten yanmalı motorlarda meydana gelen yağ kayıpları başlıca çevre kirliğine ve performans kayıplarına yol açarlar. Bu çalışmada tek tek parametrelerin ikincil bölgedeki iki piston segmanı arasındaki bölge, yağ toplanması üzerine etkileri araştırılmıştır.

Bu çalışmada yağ kalınlığının ve yağ sıcaklığının, içten yanmalı motorlarda yağ kaybı mekanizmalarına sebep olan ikincil bölgede yağ toplanması olayına etkilerinin araştırılması amaçlanmıştır. Modellenmiş piston silindir deney düzeneği üzerinde kontrollü deneyler yapılmıştır.

İkincil bölgede toplanan yağ miktarının yağ kalınlığı ve yağ sıcaklığından etkilendiği görülmüştür. İkincil bölgede toplanan yağ miktarı yağ kalınlığındaki artışla birlikte artmıştır. 45µm yağ kalınlığının altında yapılan deneylerde elde edilen sonuçlar

ikincil bölgede toplanan yağ miktarının yağ sıcaklığının artması ile birlikte arttığını göstermektedir.

Anahtar Kelimeler: Yağ kaybı, Yağ toplanması, Yağ kalınlığı, Yağ sıcaklığı, Yağ geri akışı, İçten yanmalı motorlar

To my beloved wife

ACKNOWLEDGMENTS

I wish to express my gratitude to my supervisor, Prof. Dr. Zafer DURSUNKAYA, for his guidance, advice, criticism and insight throughout the research.

I am grateful to Mechanical Engineering Department technical staff Rahmi ERCAN and Mehmet ÖZÇİFTÇİ for assisting me during experiments. I am also grateful to research assistant at Food Engineering Department Bekir Gökçen MAZA for helping and accompanying me during the oil content analysis.

I owe a special thank to my parents for supporting me throughout my entire life. I also would like to thank my parents in law for their precious support and encouragement.

I would like to express my gratefulness to my brother Emrah for accompanying and helping me during the experiments at weekends even he had exams ahead to study.

Finally, many special thanks to my dear wife Yonca for her continuous support, motivation and patience during my thesis study as she did in every step of my life. Without her I couldn’t be able to complete my thesis study.

TABLE OF CONTENTS

LIST OF TABLES

LIST OF FIGURES

CHAPTER 1

INTRODUCTION

Oil loss mechanisms in internal combustion engines have been subject to many efforts recently. By the help of technological developments, effects of several problems due to oil losses are tried to be reduced. A spark-ignition automobile engine approximately consumes four grams of oil per hour (0.43 g/bhp-hr) and large marine diesels approximately consumes three kilograms per hour (0.37 g/bhp-hr) [21]. In diesel engines oil consumption also contributes to exhaust particulate matter (PM).

Oil losses occurred in internal combustion engines cause mainly two problems as environmental pollution and performance losses. The amount of oil available in the internal combustion engines has implications on power loss, wear of cylinder components and loss of piston-ring performance. Besides, it has been shown that engine oil is a major contributor to the burned and unburned hydrocarbon emissions. In order to prevent the environmental pollution, strict regulations on automobile engines were ruled. These regulations increased the importance of oil loss mechanisms as a research topic in order to understand the phenomena and solve the problem that causes the performance losses in internal combustion engines and environmental pollutions.

1.1. Oil Loss Mechanisms in Internal Combustion Engines

It has been well shown experimentally that two main oil loss mechanisms exist. These are due to valve train and in cylinder components.

1.1.1. Oil Loss Due to Valve Train

Lubrication of the valve train components; which are rocker arms, valve springs, push rods, lifters and cam mechanism; is important for the sake of reducing engine friction and power losses. It has been shown that 15-25 % of total oil loss is due to valve train [1].

1.1.2. Oil Loss Due to In Cylinder Components

Piston and ring design has a great effect on oil consumption. Effects of design on oil consumption are well known but still need further investigations especially regarding the effects of individual parameters. Studies on oil loss mechanisms showed that 75-85 % of total oil consumption is due to in cylinder components [1]. Oil loss due to in cylinder components consist of three different sub-mechanisms. These sub-mechanisms are evaporation, scraping and blow back of oil.

Due to reciprocating movement of the piston some oil is still present on the cylinder wall prior to combustion. Some of this oil evaporates during the combustion and mixes with the combustion chamber products accounting the 5-10 % of total oil consumption [2].

During the upward motion of the piston, top compression ring scrapes the oil to the combustion chamber starting from the bottom dead center (BDC) position. The oil accumulated on the top compression ring is spread over the combustion mixture during the expansion due to inertia effects.

The final mechanism is the blowback of engine oil. The oil present in inter crevice volumes is entrained into the combustion chamber by the blow-by gases. This mechanism will be investigated in this thesis study.

1.1.2.1. Oil Loss Due to Oil Blowback

For a typical 4 stroke diesel engine; three rings make up two crevice volumes by dividing the space between the piston and cylinder inner surface. A representation of these volumes is shown in Figure 1.1. It is shown that inter ring crevice volumes and pressures have a significant effect on oil blow back [3, 4, 5].

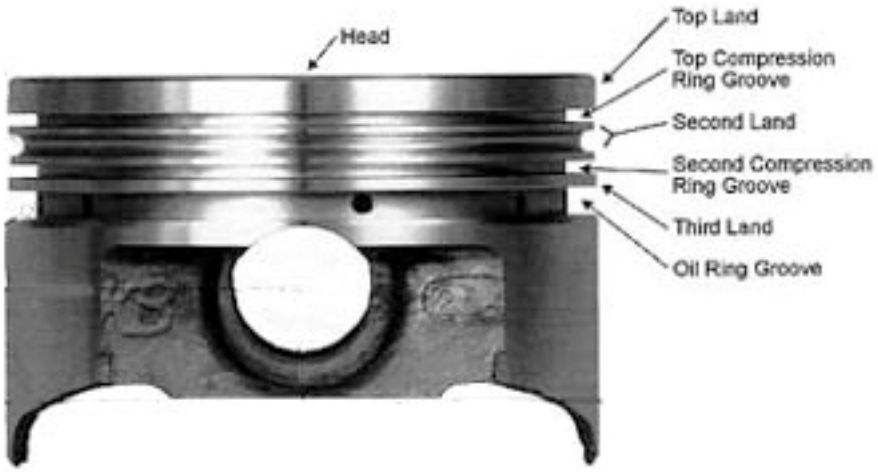

Figure 1.1 Piston and ring grooves

Existences of two oil flow paths have been shown [6, 7]. In Figure 1.2 Thin lines in the schematic representation represent the minor flow path. Due to the deformations during operation, cylinder bore becomes non circular and the oil in the 2nd land flows through top ring into the combustion chamber. However as technology develops, this oil flow path becomes negligible. In Modern IC engine designs, the distortion of the cylinder wall reduced and the secondary motion of the piston is well controlled.

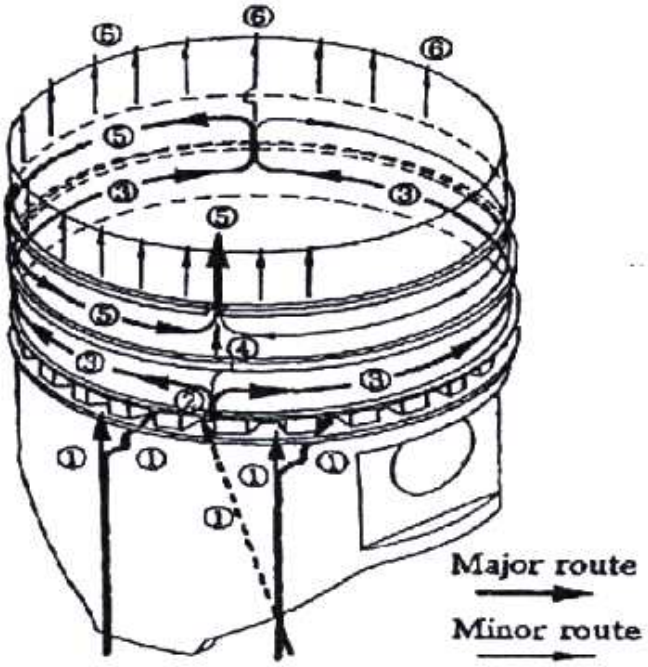

Figure 1.2 Oil flow paths [7]

Thick lines in Figure 1.2 represent the major flow path. Some of the recent studies consider the space between the ring end gaps as the main oil passage [3, 5, and 7]. This passage is shown in the Figure 1.3.

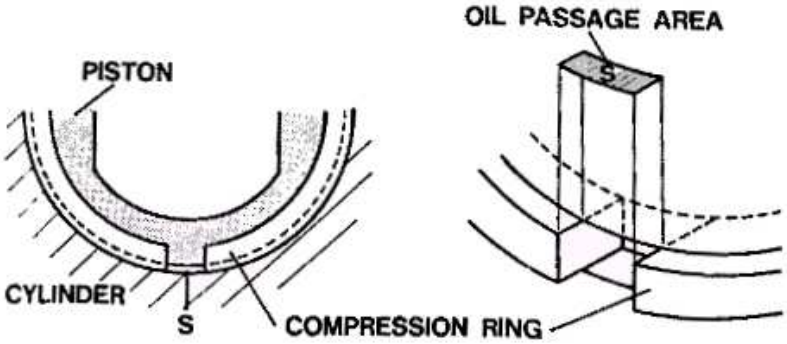

Figure 1.3 Gas and oil main passage area [8]

The reason of the gas flow is the pressure variation, shown in Figure 1.4 , between the inter ring crevice volumes. Oil is accumulated in the 2nd land during the compression and early expansion strokes due to the high pressure in the combustion chamber relative to the 2nd land. Gas flow at sonic speeds occurs to the 2nd land as a result of this pressure difference. The entrainment of the oil on the cylinder wall into the 2nd land as oil mist occurs during this gas flow. The oil mist flows into the combustion chamber when the cylinder pressure drops below the inter ring pressure due to rapid expansion and depressurization. In Figure 1.5 oil blowback mechanism is represented schematically.

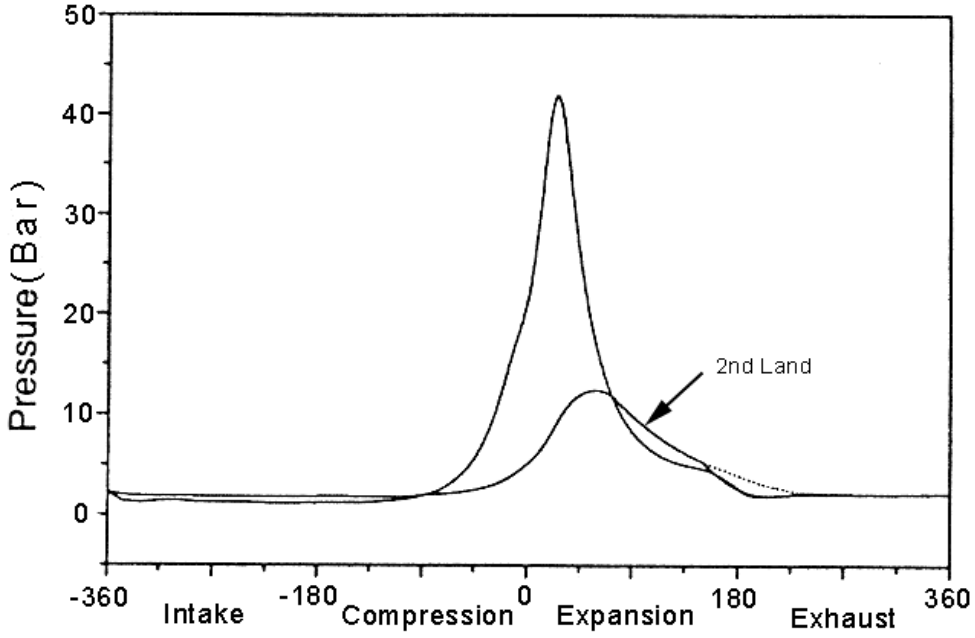

(a)

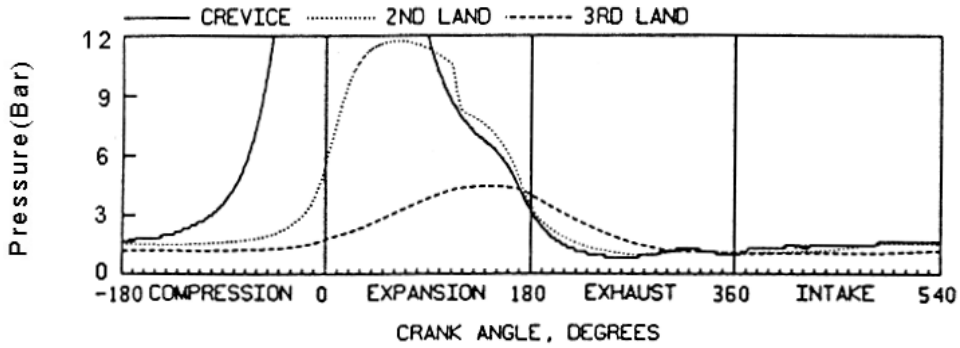

(b)

Figure 1.4 a) In cylinder pressure variations b) 2nd land pressure variation [13]

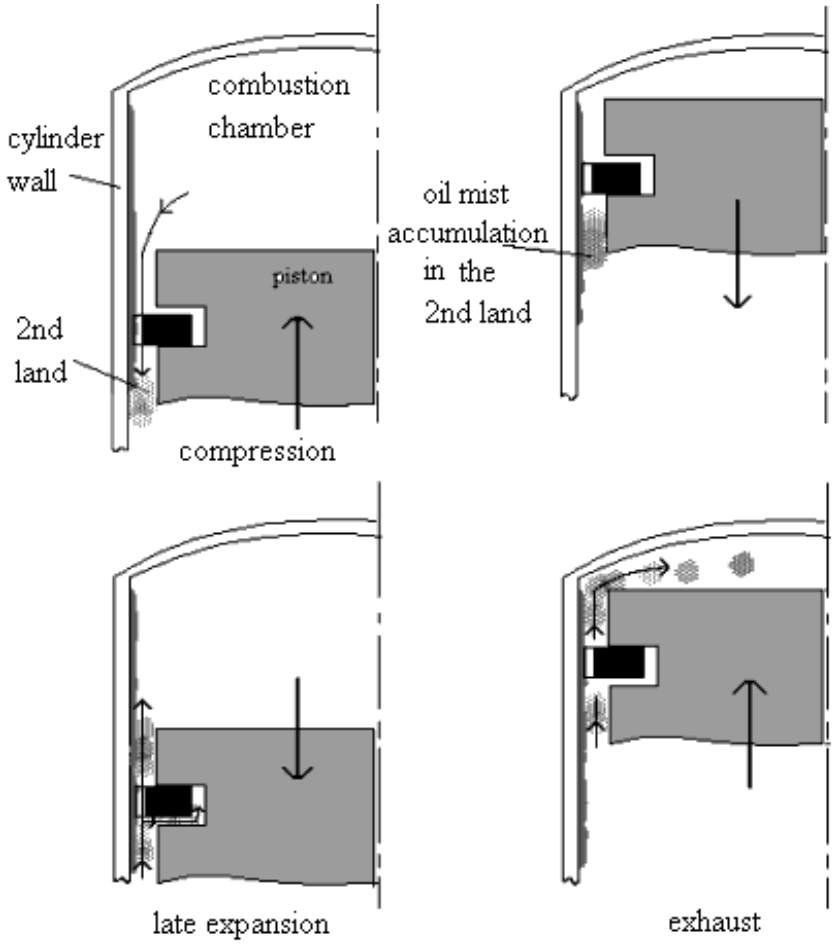

Figure 1.5 Schematic representation of oil blowback mechanism

The outflow of the oil mist from the piston-ring crevice to combustion chamber during the post-flame period (later stages of expansion stroke and during the exhaust stroke) was observed by Green and Cloutman [19] using a planar laser induced fluorescence (PLIF). Figure 1.6 shows the outflow from the 2nd land at a position away from the top ring end gap and Figure 1.7 shows the outflow at the top ring end gap.

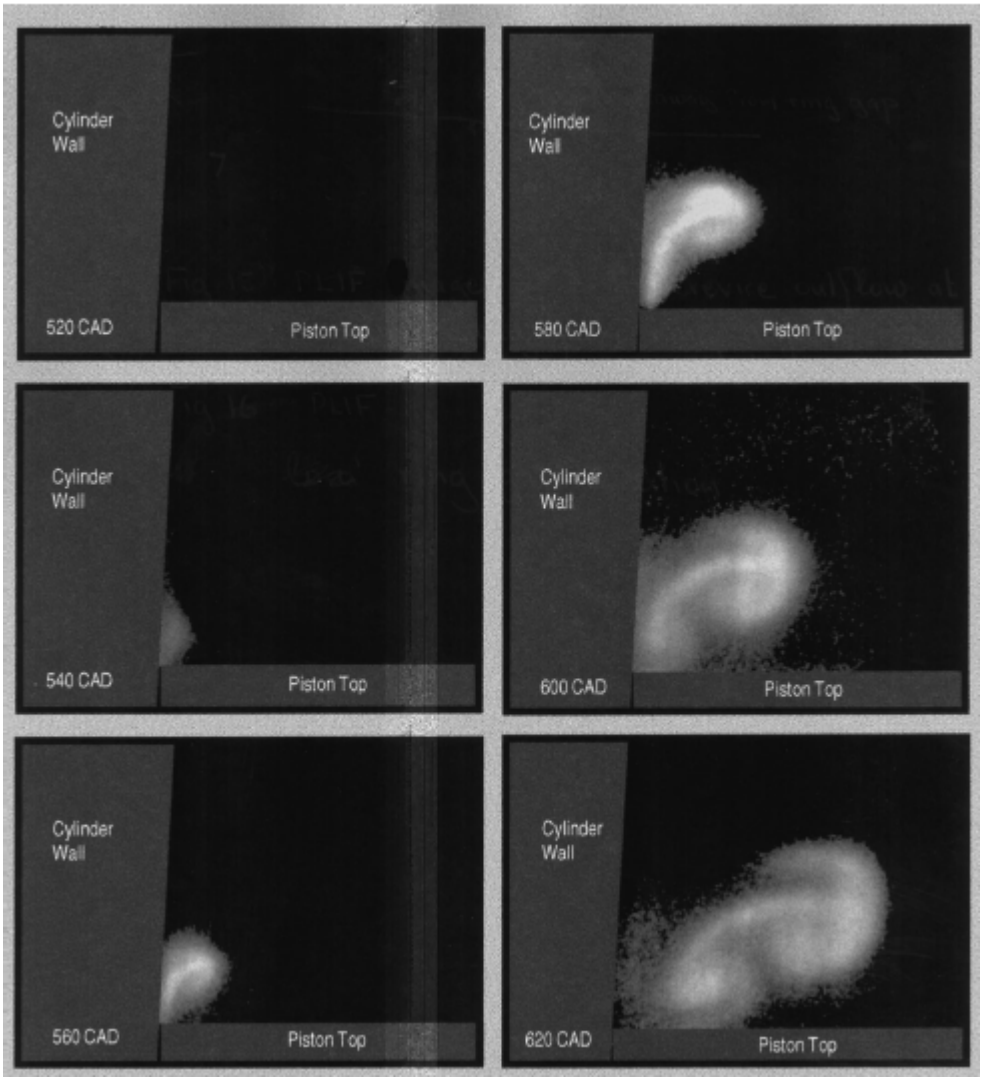

Figure 1.6 PLIF images of piston crevice at location away from top ring end gap [19]

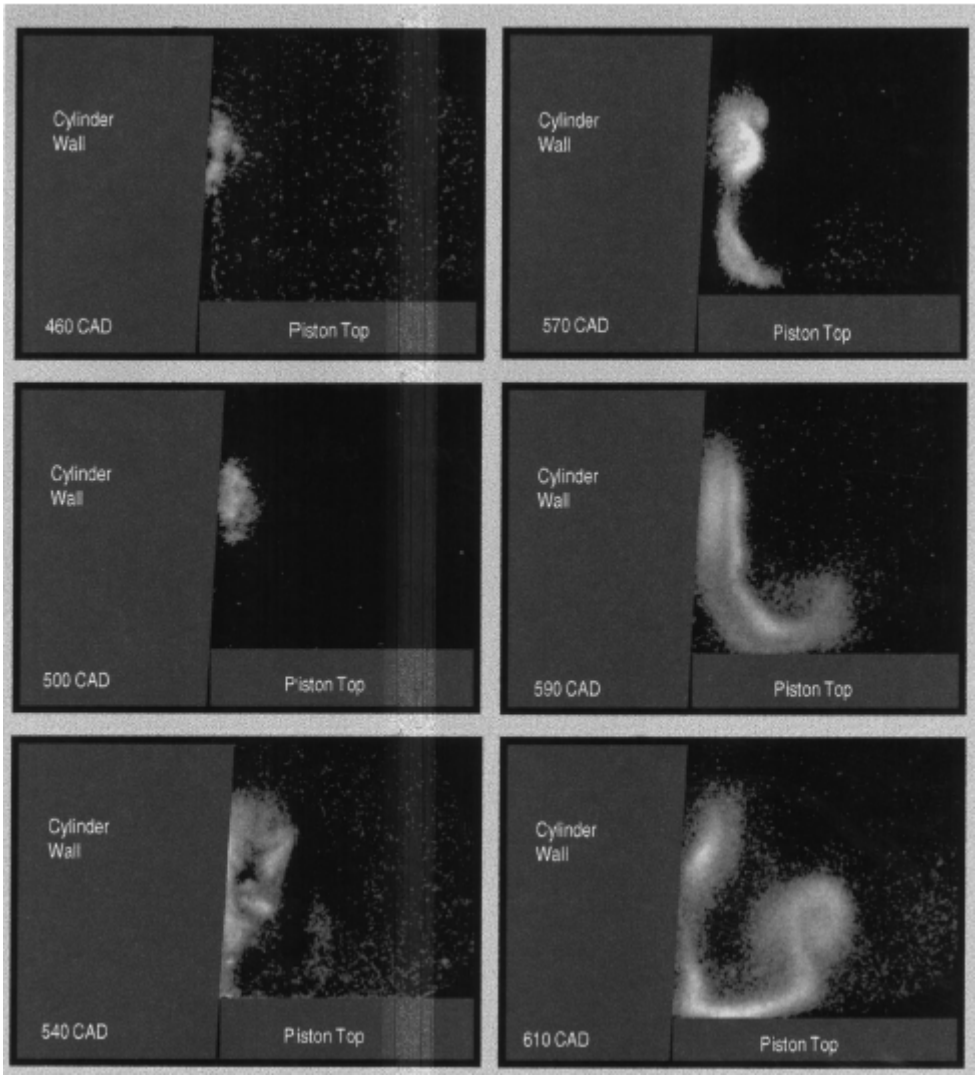

Figure 1.7 PLIF images of piston crevice at top ring end gap [19]

Hoult and Shaw [18] advanced the "Puddle Theory of Oil Consumption" which related the oil consumption to the 2nd land film thickness and reverse flow through the top ring end gap. Shaw validated the theory with direct measurements of oil consumption in a Kubota engine with pinned rings. In this study; oil film thicknesses were measured by laser induced fluorescence techniques. It was stated that oil accumulated in the 2nd land is strongly depended on the velocity of the blow-by gases over the oil puddle under the top ring end gap, the depth of the puddle, surface tension and viscosity of the oil. The geometry related to the theory is shown in Figure 1.8 [18].

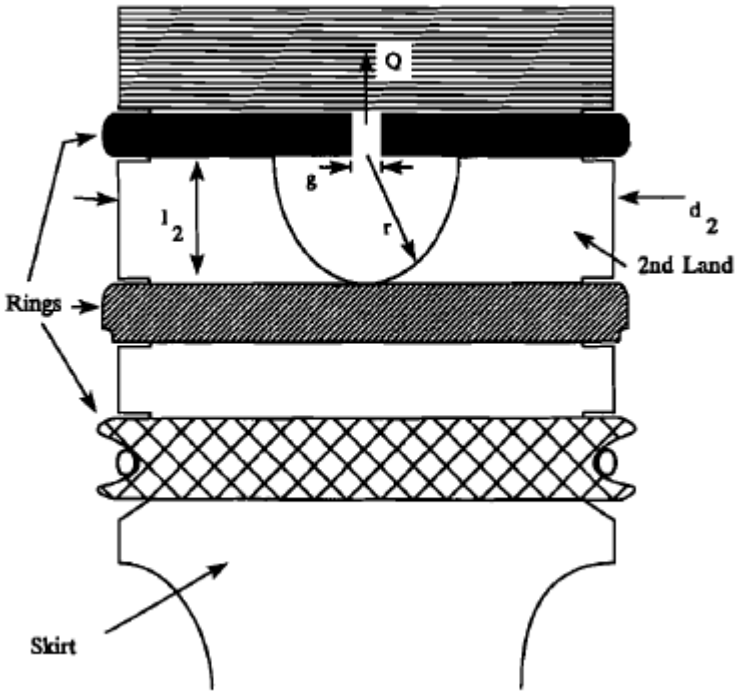

Figure 1.8 Side view of piston, showing dimensions relevant to oil consumption [18]

Entrainment of oil into blow-by gases can be explained by two phase flow of gas and liquid. For the blowback mechanism, the gas moving over the liquid due to pressure difference causes formation of droplets by tearing the liquid from interface. The amount of oil entrained due to this mechanism is affected by the flow conditions and physical properties of the fluids. Hewitt and Hall-Taylor [9] summarized the entrainment mechanisms based on experimental observations. Droplets can be formed either by breaking up of waves created on the liquid surface during the gas flow or by the emission of a bubble from a liquid surface. Wave undercutting and shearing off of roll wave crests were presented as the main mechanisms encountered in liquid entrainment. They emphasized the strong dependence of droplet entrainment on gas-liquid flow combinations, geometry, and physical properties such as surface tension and viscosity. Five basic entrainment mechanisms are shown in Figure 1.9 [9].

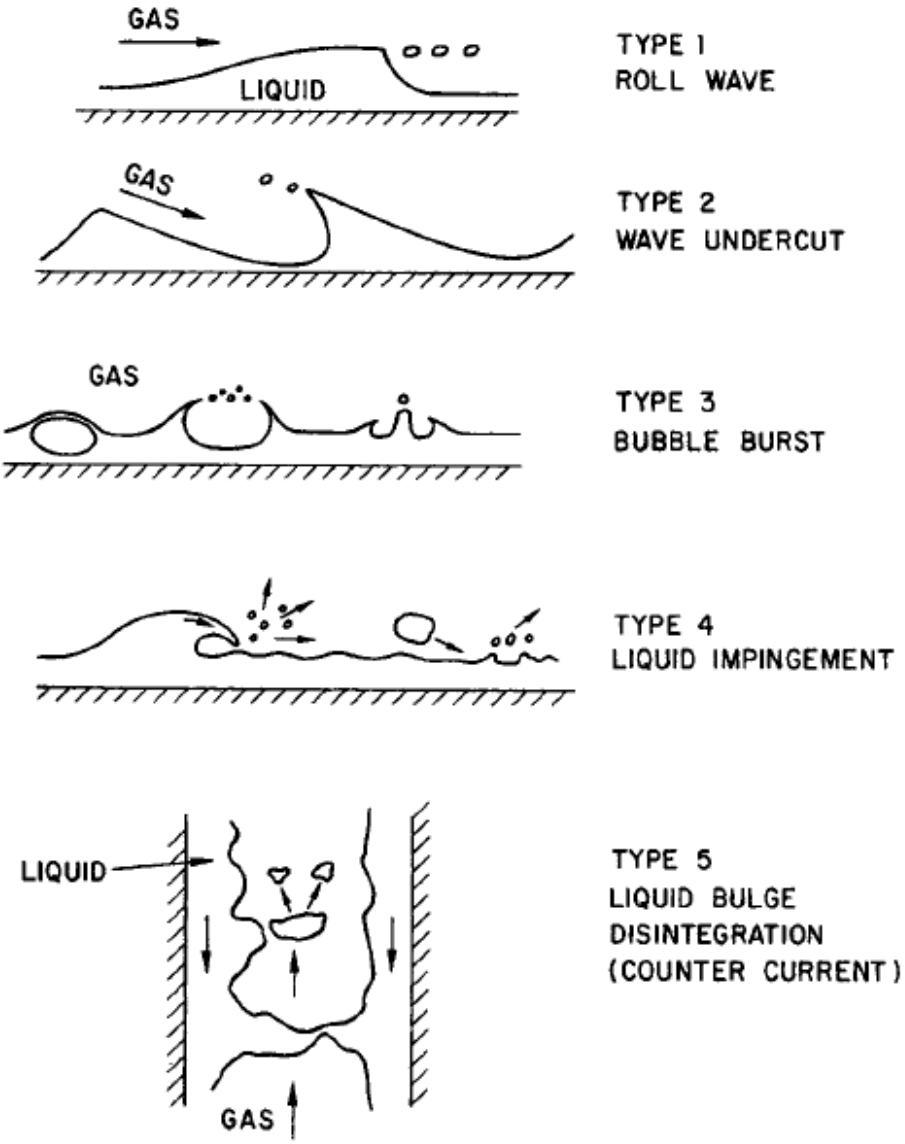

Figure 1.9 Entrainment mechanisms [9]

Ishii and Grolmes [16] developed inception criteria for droplet entrainment in two-phase flow. They concluded that applicability of mechanisms depends on the flow conditions, and abrupt changes observed in the experiments were attributed to a change in the entrainment mechanism.

Ishii and Mishima [17] developed correlations for the entrained fraction of water in the water-air system and used the same two mechanisms in their model. Their results showed that the prevailing entrainment mechanism changes with Reynolds number.
There are some accepted methods used in measurement of oil consumption in IC engines. “Weight method” and “sulfur trace method” are the two common methods used for oil consumption measurements. “Weight method” can be defined as measuring the weight of oil before and after the engine operates. “Sulfur trace” method is based on tracing the sulfur in the lubricating oil by means of detecting the SO_2 concentration in the exhaust gas.

Lizumi and Koyama [10] developed a method to measure the oil consumption of a diesel engine using sulfur tracing (S-trace), which was based on the detection of SO_2 in the exhaust gas. For this purpose they used a flame photometry detector analyzer to measure the SO_2 concentration in the exhaust gas and accordingly estimate the oil consumption in transient operation of the engine.

Researches have so far intended to study the gross effects of certain geometric parameters such as ring end gap positions, piston ring face profile on this particular mechanism. But the effects of individual parameters, such as oil film thickness, kind of lubricant; temperature and pressure are still unknown.

Saito, Igashira and Nakada [8], used a transparent glass cylinder engine in order to clarify the oil loss mechanism via piston rings. They used a system composing of a high speed camera and a TV camera with a synchro flash and synchro memory. They injected colored oil from various points on the piston surface and the oil movement around the piston rings was analyzed. They concluded that high vacuum inside the cylinder drew oil up into the combustion chamber through the joint gaps in the compression rings as the main pass. They also proposed that the quantity of the oil in the third land was small and did not penetrate to the second land or the top land, therefore did not contribute to the oil consumption.

Wong and Hoult [11] studied the lubricant film characteristics and oil consumption in a small diesel engine experimentally, using a radioactive tracer for the oil consumption and laser fluorescence diagnostics for the film thickness measurements. The study showed that oil film thickness affected the oil loss in diesel engines. They could not, however, find conclusive evidence that the amount of oil in the second land correlated with the oil consumption. In addition, their results showed that the crown land, the volume between the top compression ring and top surface of the piston, ran dry and therefore could not contribute to oil consumption in any significance.

Kim et al. [7] studied the importance of inter-ring crevice volume as a source of unburned hydrocarbon emissions numerically. A physical flow model integrated with a ring dynamics model to predict the gas flows through the inter-ring crevice was constructed. The results showed that late in the expansion stroke some of the interring mixture returned to the combustion chamber. Moreover, they found that the unburned hydrocarbon HC emissions caused by the inter-ring mixtures were 10%–30% of the entire unburned HC emissions over an engine speed range of 1250–3500 rpm and the reduction in emissions was closely related to blow-by, which was directly related to the volume of the inter-ring crevice.

Chun [23] worked through “The Puddle Theory of Oil Consumption” and developed a simulation program to calculate the oil loss in internal combustion engines. The results later compared with the real oil consumption data and concluded that the developed computer program real time condition of an engine in terms of oil consumption could be predicted good reliance

İçöz [13] investigated the effects of oil thickness parameter on oil accumulation in the 2^{nd} land by constructing an experimental setup modeling the 2^{nd} land volume and combustion chamber in Cartesian geometry. This study was concluded that oil accumulation in the 2^{nd} land had been effected by the oil film thickness parameter.

1.2. Scope of Work

In this study it was proposed to investigate the effects of individual parameters such as oil film thickness and temperature on the accumulation of oil in the 2nd land volume. It was stated by Hoult and Shaw in "Puddle Theory of Oil Consumption" that the amount of oil flow to the 2nd land is directly related to the velocity of the blow-by gases, oil film thickness in the 2nd land and Taylor number of the oil. Taylor number is the ratio of the viscous forces to surface tension forces. Both viscous and surface tension forces are depended to the temperature of the fluid. In Figure 1.10; for various single or multigrade oil types kinematic oil viscosity with respect to oil temperature is illustrated [22].

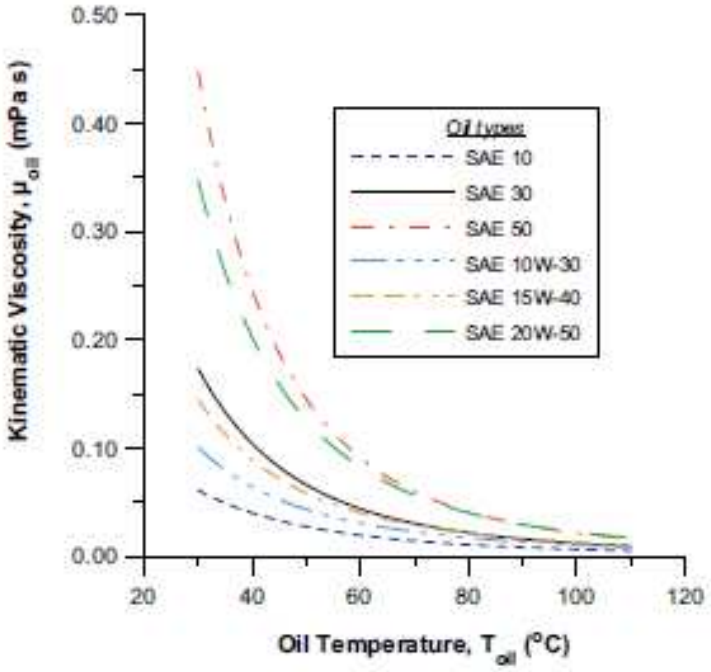

Figure 1.10 Kinematic viscosity variation with oil temperature for different types of oil

An experimental setup, which is modeling a single stroke of a diesel engine, was constructed by İçöz [13] in order to investigate the oil accumulation in 2nd land volume. A heating system added to the previous experimental setup and necessary

modifications were done on the system. UV light absorption analysis was performed on the oil gas mixture sampled from the modeled 2nd land. The results are compared with the previous studies and known oil consumption mechanisms.

CHAPTER 2

EXPERIMENTAL SETUP

The effect of individual parameters on oil blowback, such as oil film thickness and temperature, was not well studied experimentally. Gross effects of certain design parameters were aimed to investigate in most of the previous studies. İçöz [13] designed and constructed an experimental setup modeling the piston cylinder subassembly. Investigating the effect of oil film thickness is not easy on a real engine. Due to the effect of gravity controlling the oil film thickness would not be possible; in addition it wouldn't be reliable to have uniform concentration of mixture in the 2nd land. İçöz transformed the piston cylinder, interring crevices in real engines into a Cartesian geometry with similar dimensions to a diesel engine piston cylinder subassembly (Table A. 1).

Modeled piston cylinder subassembly, sudden expansion mechanical valve and free moving piston cylinder were subassemblies of the experimental setup that İçöz used. Sampling tubes, check valve, a heater and a support leg were the auxiliary components used in this thesis work. A schematic representation of the experimental setup is shown in the Figure A.1.

Experimental setup was designed according to a pressure simulation program developed by İçöz. It was aimed to investigate to reach necessary pressure ratios in order to obtain a choked and supersonic flow between modeled combustion chamber and 2nd land as it is present in real engines. . It was also shown that the experimental setup could be utilized for investigation of the oil accumulation in the 2nd land of the internal combustion engines.

2.1. Subassemblies of Experimental Setup

Piston-cylinder subassembly, sampling tubes, heater, free moving piston subassembly and sudden expansion mechanical valve consist up the experimental setup.

2.1.1. Piston Cylinder Subassembly

A modeled piston cylinder subassembly had been designed and produced in a Cartesian geometry. In the piston cylinder subassembly combustion chamber, inter ring crevice volumes and ring end gaps had been converted in Cartesian geometry. Schematic representation of the conversion of the volumes and surfaces is shown in Figure A.2.

Top plate, center plate, bottom plate, stopper, check valve and sampling tube are the main parts of the subassembly as shown in Figure A.3. Technical drawings of the experimental setup can be found in thesis work of İçöz [13].

2.1.1.1. Top Plate

Top plate, made of high carbon steel, is the upper case of the modeled piston cylinder subassembly. Main function of the top plate is stopping the free moving piston and connecting two subassemblies; free moving piston subassembly and piston cylinder subassembly. There is a disk placed on the top plate with an outer diameter of 100 mm and thickness of 10 mm which is called stopper. Stopper is the main flow area with its 40 mm diameter inner hole between PC1 and PC2.

Top plate was connected to the free moving piston subassembly by four M10 studs. There is one relief valve with a pressure gage mounted on it.

2.1.1.2. Center Plate

Center plate is the main part of the piston cylinder subassembly. Sampling chamber (SC), flow passage gap, flow separator are located on it. It is also responsible for carrying the check valve with its three identical springs and involves in constituting up PC1.

SC located, on the top plate, simulated the 2nd land. In order to get uniform gas mixture 2nd land was lumped into a narrow region. The ring end gaps were simulated by the flow passage gap with dimensions of 0.5x0.5 mm. dimensions of the flow passage gap, only passage between PC1 and SC, were same as in a real engine.

In order to obtain a uniform pressure along PC1; the mid section of the center plate was constructed as a flow separator. Flow separator was used to distribute the air on both sides of PC1 so the air would not pass through the flow gap to SC directly. Center plate is shown is Figure A.4 and schematic representation of the flow path is shown in Figure A.5.

One stroke of a four stroke diesel engine had been modeled in the experimental setup used in this study. It was aimed to investigate the oil accumulated in the 2nd land after one stroke. In order to retrieve the sample from SC for analysis constant pressure in both PC1 and SC was necessary. The check valve was constructed for this reason. With the help of three identical springs; check valve was design to open only at the peak pressure in PC2, which were nine bars. The check valve was closed automatically after the free moving piston hit the stopper in order to provide a constant pressure in PC1. A schematic representation of the check valve operation is shown at Figure A.6.

2.1.1.3. Bottom Plate

Primary function of the bottom plate was simulating the cylinder wall. For the controlled experiments on oil film thickness the oil was spread on the upper surface of the bottom plate. The oil film thicknesses were controlled by the amount of oil spread on the surface of the bottom plate. All three plates were connected each other by eight M14 studs. The sealing between each plate was provided by o-rings.

2.1.2. Sampling Tubes

The oil accumulated in SC was collected through sampling tubes for UV light absorption analysis. For this purpose sampling tubes having an internal volume of 3.1cc were used. The sampling tubes were manufactured from brass and had two spherical valves on both sides in order to keep the pressurized gas inside. The picture of a sampling tube was shown in Figure 2.1.

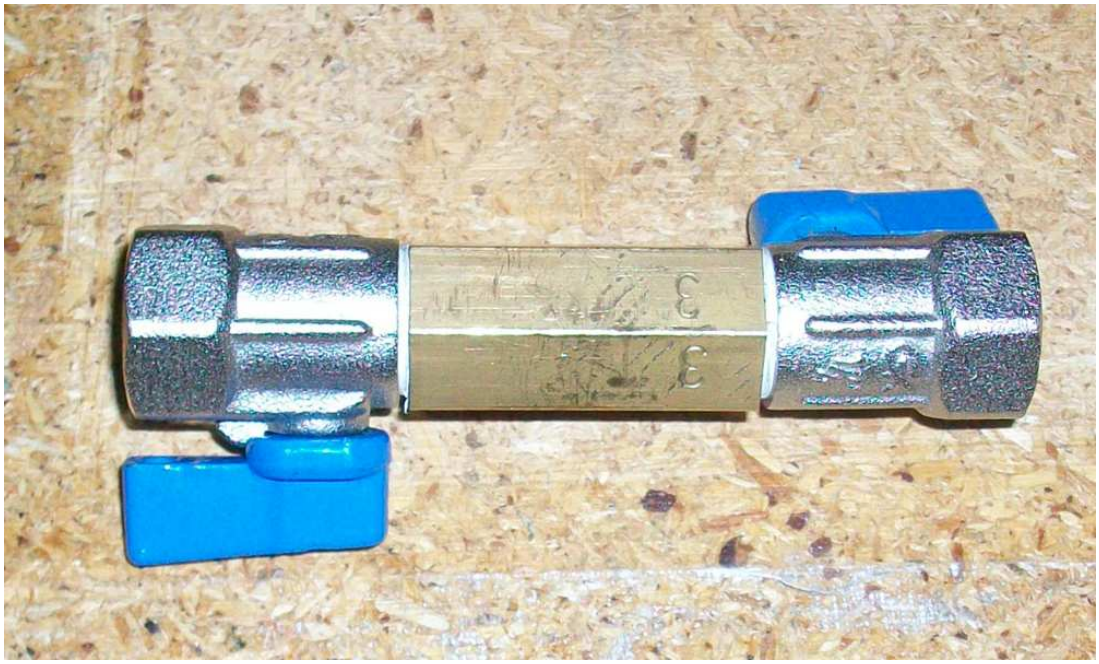

Figure 2.1 Sampling tube

2.2. Free Moving Piston Subassembly

Free moving piston subassembly was modified from a single cylinder of an OTOSAN DOVER engine block. The cylinder had a 104.7 mm diameter and the piston had two compression rings and one oil control ring. The cylinder block and the piston were modified to desired geometries. Unnecessary parts of the both piston and cylinder were removed. Pictures of the free moving piston subassembly connected to the top plate were shown in Figure 2.2.

It was calculated that a piston with 2 rings and a thickness of 24.7 mm would satisfy the experiment needs [13]. The original piston had been modified to desired geometry. Due to the necessity of undesired depressurization of PC1 through ring end gaps, two o-rings were placed around the modified piston.

Figure 2.2 Free moving piston subassembly mounted on top plate

2.3. Sudden Expansion Mechanical Valve

In the experiments in order to achieve the conditions similar with the combustion process in a real engine, rapid pressurization of the free moving piston cylinder subassembly was needed. It was decided to use a sudden expansion valve in the experiments among several alternatives.

In 1970 the valve was designed and manufactured as a part of a shock tube. Originally it was intended to be used as a substitute for the diagram in the construction of a shock tube. Driver section of the shock tube was adapted to the experimental setup by means of some modifications without changing the original construction.

Gas storage chamber (GSC), activation chambers and the mechanical valve were the main parts of the driver section of mechanical operated shock tube. Moving the piston due to high pressure difference was the operating principle of the mechanical operated shock tube. Activation chamber and GSC were pressurized initially to identical pressures when the valve was still being closed. The solenoid valve connected to the activation chamfer opens the valve and the pressure of activation chamber drops to atmospheric pressure. At this time due to the force resulted from the pressure difference of activation chamber and GSC, piston starts moving at the same time opens the flow passage area by releasing the air inside the GSC. Opening time of the piston depends on the pressure difference exerted on the piston. For 10 bar of driver section pressure piston opening time was found to be 0.5 msec [15].
Gas storage chamber volume was initially 13 liters. In order to avoid any damage on the subassemblies, sudden expansion mechanical valve was modified to have less volume inside. Modifications were done by filling the excess volume by polyamide. Schematic representations of the sudden expansion mechanical valve before and after modification were showed in Figure A.7.

2.4. Modifications on the Experimental Setup

In this thesis work; it was aimed to investigate the effect of oil film thickness and temperature on the amount oil accumulated in 2nd land. In order to provide necessary heat for controlled experiments and to control the oil temperature, a heater and three thermocouples installed to the system as seen in Figure 2.4.

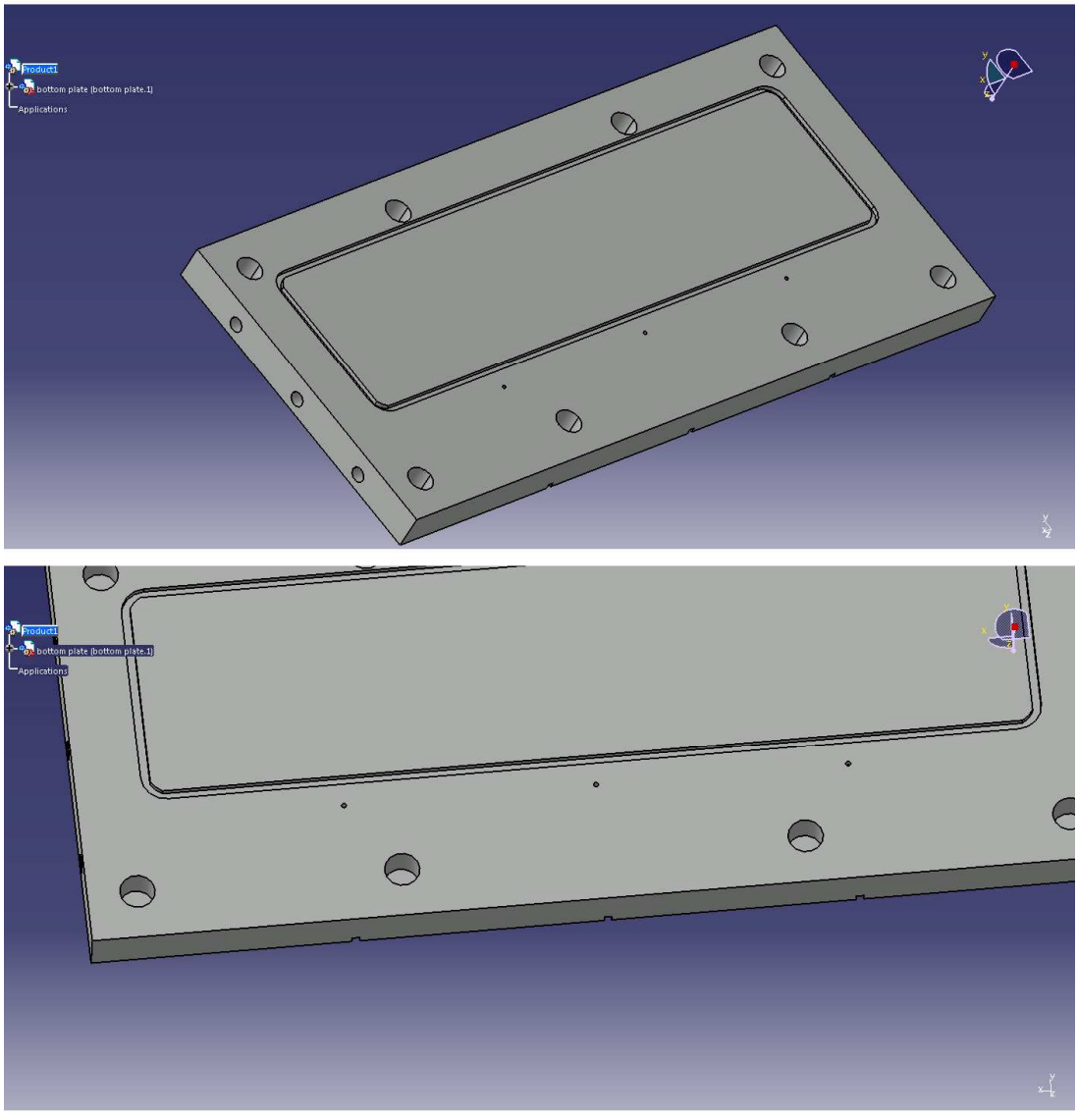

Figure 2.3 Thermocouple holes drilled through the bottom plate

Figure 2.4 Bottom plate with thermocouples installed

Three holes were opened through bottom plate in order to place the thermocouples inside as shown in Figure 2.3. All three thermocouples fixed on the bottom plate and sealed as they would be on contact with bottom plate's surface. On the bottom surface of the bottom plate, channels were opened in order to prevent direct touch of the thermocouple cables to the heater. Three dimensional demonstration of the channels mentioned were shown in Figure 2.5. All of the thermocouples were insulated against the direct heat that might come from the heater as seen in Figure 2.4.

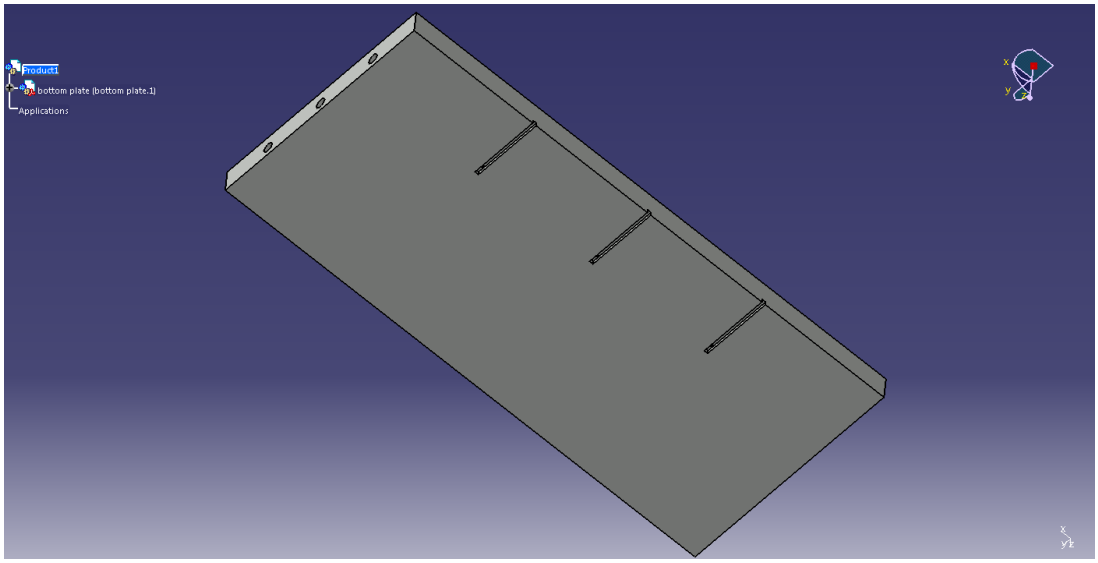

Figure 2.5 Channels opened on the bottom surface of bottom plate

During the experiments, for heater not to damage from the force excited by the free moving piston, six M8 studs were placed on the side walls of bottom plate. The force excited by the free moving piston was calculated and necessary analyses were made by commercial finite element solver software for the sake of not rupturing the bottom plate.

The graphical outputs of the finite element are given in Appendix-B. Technical drawing of the bottom plate after the necessary modifications is given in Appendix-C.

The force exerted on the plate was estimated by the pressurization simulation program routine written by İçöz [13]. According to the results the velocity graph of the free moving piston was shown in Figure 2.6.

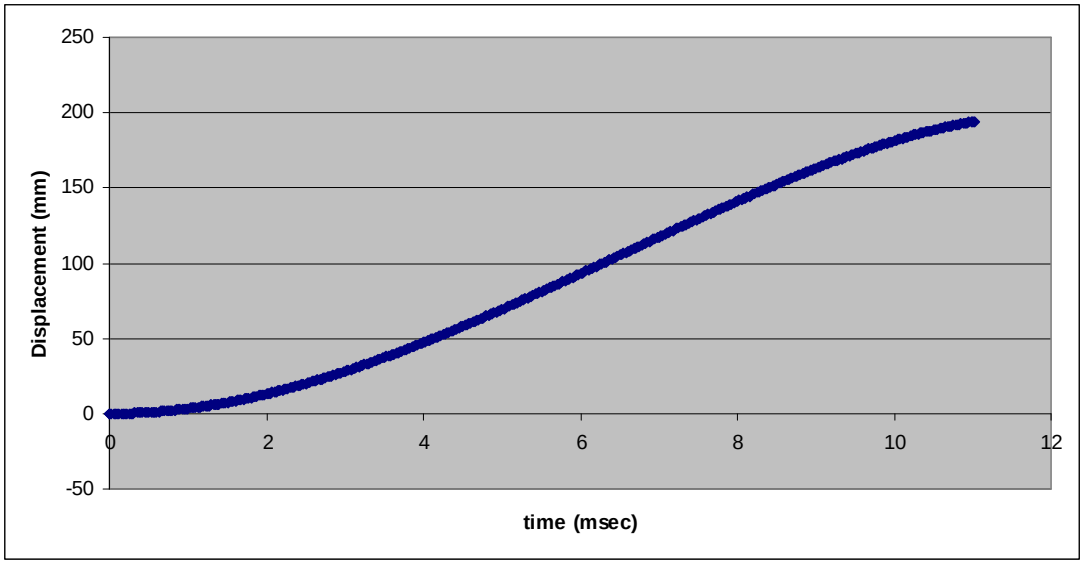

Figure 2.6 Displacement of the free moving piston

Taking the derivative of displacement of the free moving piston twice; acceleration of the free moving piston was found as in Figure 2.7.

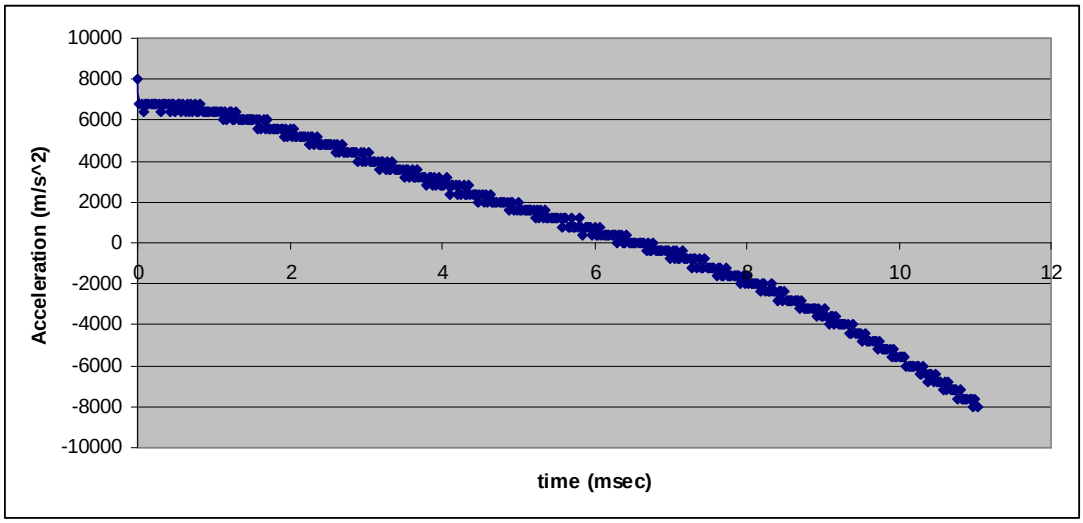

Figure 2.7 Acceleration of the free moving piston

Mass of the free moving piston was 0.575 kg. Maximum force exerted on the experimental setup by the free moving piston was 4600 N. Including a safety factor of 1.74 , finite element analysis for the static force on the bottom plate were performed for 8000N. According to the analysis results it was shown that bottom

plate and the M8 studs would not rupture due to the force exerted on the experimental setup after the stroke of the piston.

2.5. Experimental Setup Assembly

Base of the experimental setup assembly is formed by the piston cylinder subassembly. The heater was located under the piston cylinder subassembly by touching the lower surface of the bottom plate in order to supply the necessary heat. The heater was hold in position by a support which enabled simple operation during the assembling and disassembling phases of the experimental setup. Top plate of the piston cylinder subassembly was connected to free moving piston subassembly by keeping the stopper inside. Free moving piston subassembly connected to the sudden expansion mechanical valve by 90º elbow. Three thermocouples placed on the bottom plate were read by help of the voltage display unit. Three pressure gauges were used on the setup, in order to see the pressure on the specified volumes (Figure 2.8). Pressures in GSC, activation chamber and PC1 were checked during all experiments. Experimental subassembly was shown in Figure 2.9.

Pressurization characteristics of the PC1 and SC were shown to matched to desired pressurization characteristics [13] as in Figure 2.10. In the previous work with this experimental setup it was measured that the gas flow into SC was lasted about 17 ms [13]. The duration of gas flow into 2nd land corresponded to an engine operating at 3000 rpm. For a larger portion of the process pressure ratio of PC1 and SC were above 2, which provided a sonic and choked flow as it was aimed.

(a)

(b)

Figure 2.8 Pressure gauges used for (a) monitoring PC1 (b) GSC and activation chamber.

Figure 2.9 Experimental setup assembly.

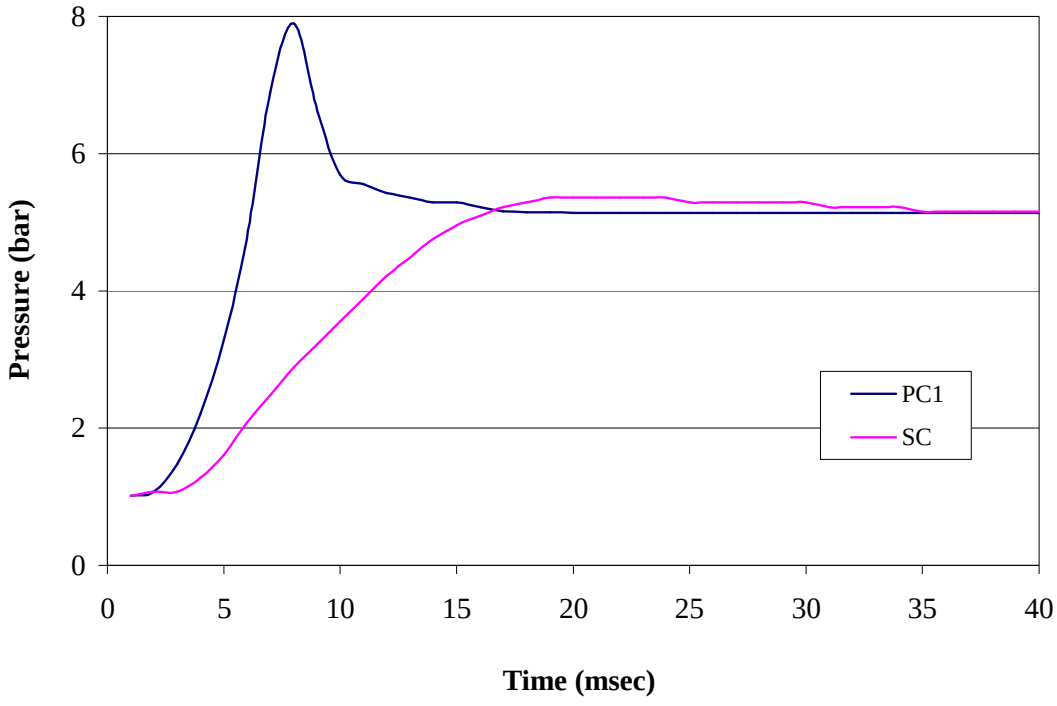

Figure 2.10 Experimental pressure variations in PC1 and SC [13]

CHAPTER 3

EXPERIMENTAL INSTRUMENTATION

Experimental instrumentation involves pressure gauges, thermocouples, voltage displayer, pipettes, UV light absorption spectrometer and solenoid valve. Solenoid valve was used for the rapid activation of the mechanical valve. Pressure gauges were employed in measuring the pressures inside the GSC, PC1 and activation chamber. Pipettes were used for measuring the amount of oil spread on the surface of bottom plate for desired oil film thicknesses. They also used for measuring the amount of hexane in the sampling tube prior to the experiment and after the experiment again used for the dilution process for necessary analysis. After an experiment the amount of oil gas mixture volume ratio was analyzed by a UV light absorption spectrometer. For the experiments of desired oil temperature the voltage was adjusted by a variac transformator in order to control the temperature of the oil. Temperatures were read by three thermocouples placed on the surface of bottom plate. The voltage difference of the thermocouples and the ice-water mixture were read by help of a voltage displayer.

3.1. Pressure Gauges

Pressure of the GSC and activation chamber was measured by means of two pressure gauges. These gauges were mounted at the gas inlet of GSC and activation chamber and the connections were sealed for the sake of any leakage as shown in Figure 3.1. These pressure gauges had a measurement range of 0-16 kg/ cm^2 with a sensitivity of 0.5 kg/ $cm^{2.}$

Third pressure gauge was mounted on the pressure relief valve of the PC1 as shown in Figure 3.2. This gauge had a measurement range of 0-16 kg/ cm^2 with a sensitivity of 0.5 kg/ $cm^{2.}$

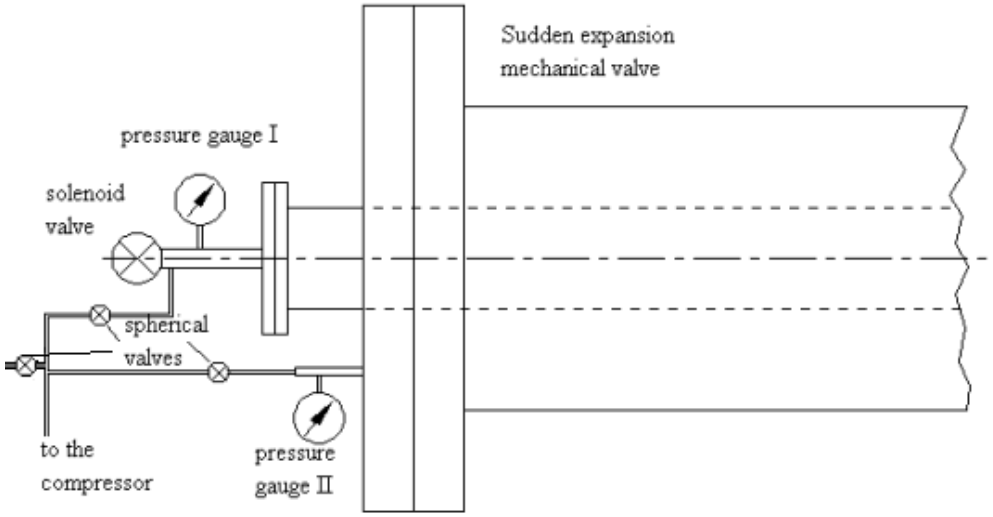

Figure 3.1 The mounting of the gauges to the sudden expansion mechanical valve

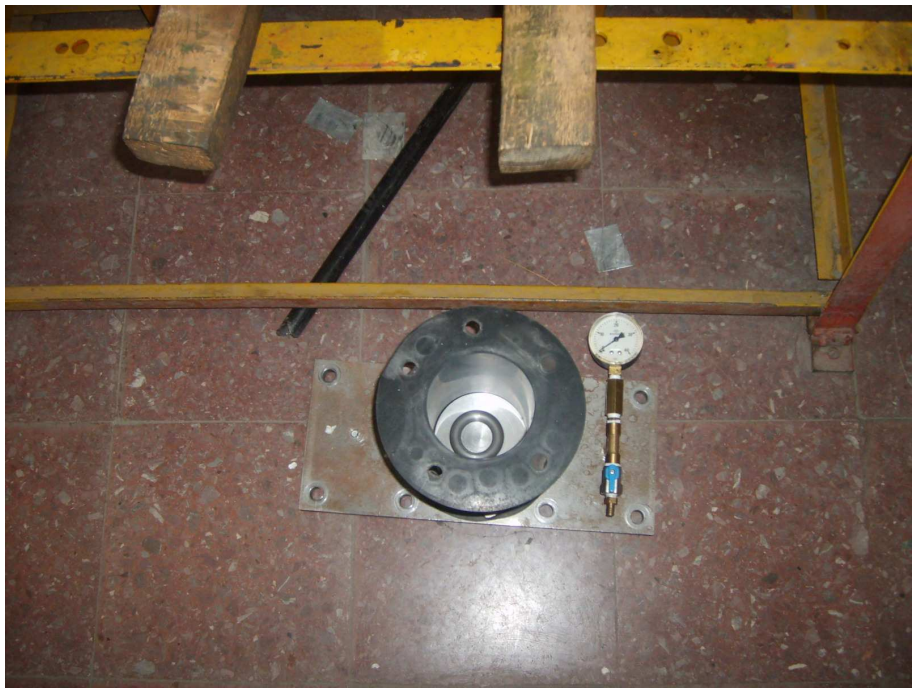

Figure 3.2 Pressure gauge mounted at the pressure relief valve

3.2. Solenoid Valve

Depressurization of the activation chamber of the sudden expansion mechanical valve was done by the solenoid valve. An electromagnet operated by 220 Volts controls the shutter for the operation of the solenoid. When no voltage applied to the solenoid valve, it is closed and there is no gas flow from the activation chamber to the ambient.

3.3. Pipettes

It was important to achieve a good accuracy for the volume measuring operation in these experiments. The oil was spread on the surface of the bottom plate measured prior to experiments in order to achieve the desired oil film thicknesses. The amount of hexane in the sampling tube was measured and then put into the sampling tube prior to experiments. Also for UV light absorption spectrometer analysis and while forming the calibration curve for UV analysis these pipettes were used for measuring the volume of the oil, hexane and oil-hexane mixture. During the experiments volumes were measured by two different scaled pipettes. One of the pipettes had a measurement range of 10-100 µl. Maximum inaccuracy was ±1.6% and the imprecision was less than 0.8%. Second pipette had a range of 100-1000 µl. Maximum inaccuracy was ±1.6% and the imprecision was less than 0.8%. The second pipette was borrowed from the Food Engineering Department of Middle East Technical University. The second pipette was used to measure the large volumes of hexane for the analysis of the sampled mixtures and forming the calibration curve for desired volume ratios of oil hexane mixtures.

Desired volume to intake into tip by the pipette was adjusted by the calibration knob. After intake the tip could be removed by the ejector button. Pictures of the pipettes are shown in Figure 3.3.

Pipettes were calibrated in the laboratory of the Food Engineering Department. The calibration was done by taking a predefined volume of pure water into the tip and measuring the weight. This process was repeated for several volumes.

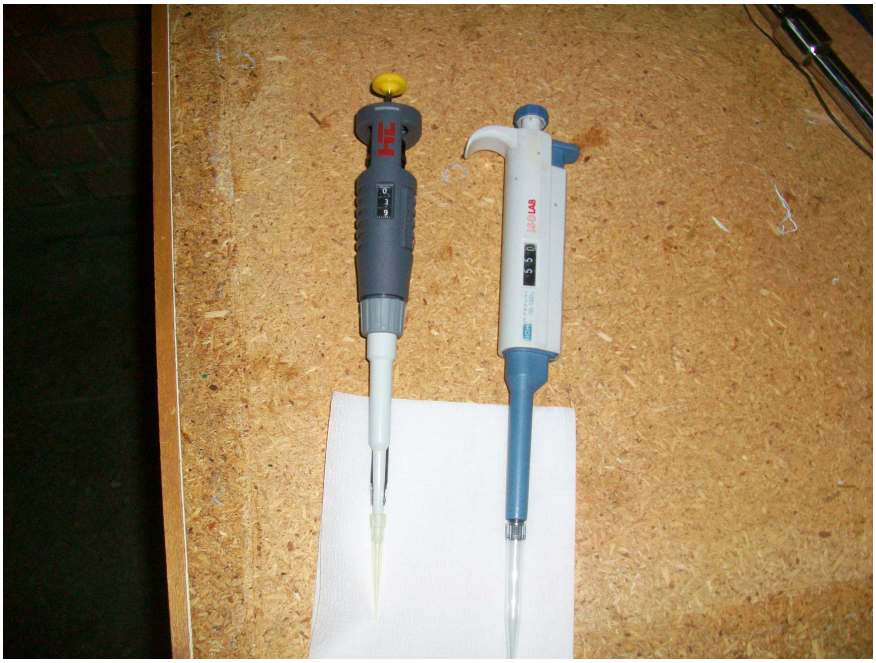

Figure 3.3 Pipettes

3.4. Variac Transformator

Variac transformator which belonged to the inventory stock of the Fluid Mechanics Laboratory was used to adjust the voltage supplied to heater. During the experiments variac transformator was adjusted to voltage values between 80 – 100 V in order to maintain the necessary heat for the experimental setup.

3.5. Thermocouples and Display Unit

A heater was installed to the experimental set up in order to control the oil temperature. Temperature of the oil was measured by means of three thermocouples placed on the top surface of the bottom plate as shown in Figure 3.4. By the help of thermocouples temperature of the bottom plate surface was measured and the

necessary heat was adjusted by means of variac transformator which controlled the voltage supplied to the heater.

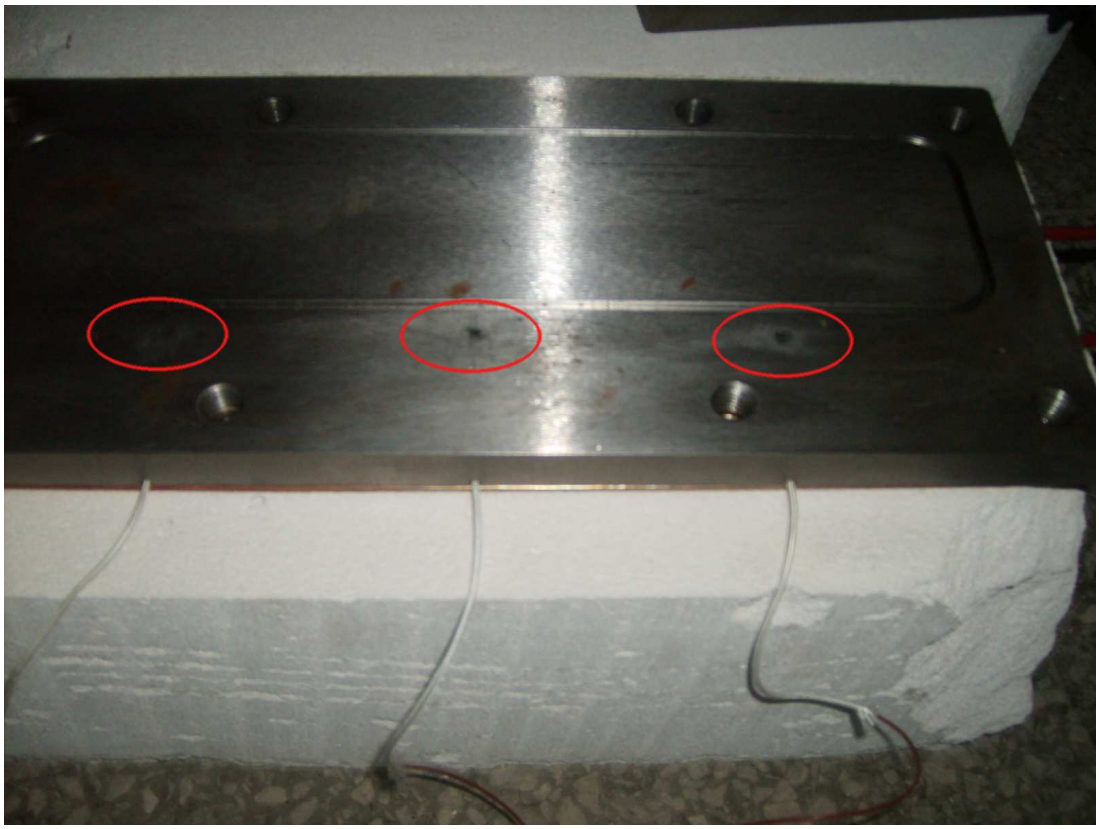

Figure 3.4 Thermocouples placed on bottom plate surface

Thermocouples used in the experimental set up were “T type” thermocouples which were made of copper alloy. As T types thermocouples were suited for measurements in the −200 to 350°C range they were enough to cover the temperature range of this thesis work. Temperature of the oil was calculated by the formula given in Equation 3.1.

$$T = 23.46V + 2.35 \qquad 3.1$$

3.6. UV Light Absorption Spectrometer

The gas mixture retrieved through the sampling tubes after the experiments were analyzed for the contents of the mixture in Food Engineering Laboratory by means of measuring UV light absorption index of the sample. A UV spectrometer belonged to Food Engineering Laboratory inventory stock, shown in Figure 3.5, was used to analyze the content of the sample.

In order to analyze the content of mixture, calibration curves for the oil hexane mixtures were formed. Three curves were formed for 283 nm wavelength for different volume fractions of hexane and oil. The results of three calibration curves were given Appendix-D. The resulting average of the three curves was shown in Figure 3.6.

Figure 3.5 UV light absorption spectrophotometer

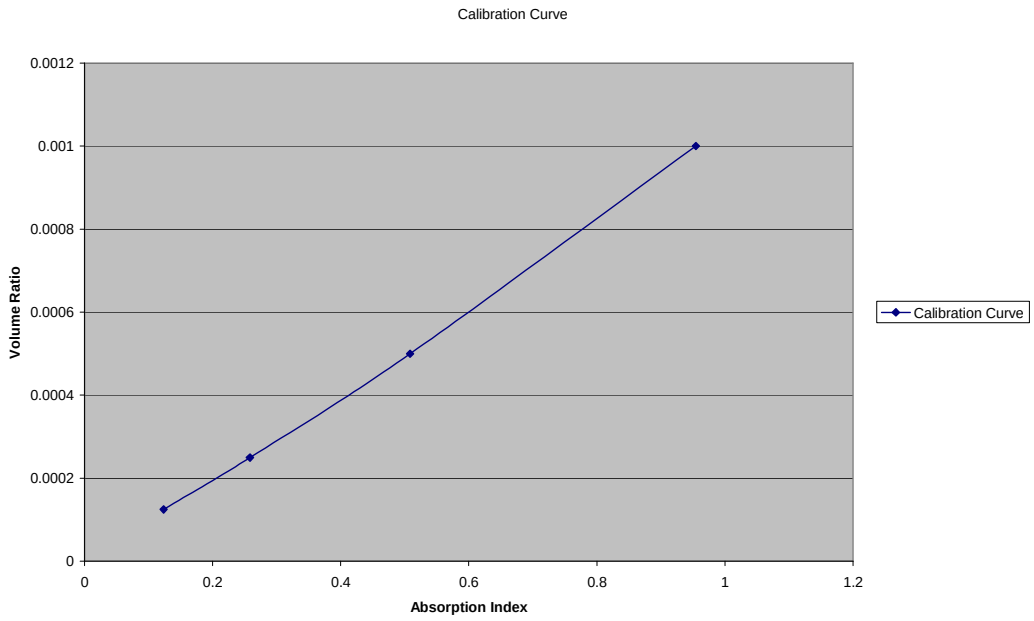

Figure 3.6 Average of three calibration curves

3.6.1. Absorption Cells

Absorption cells are used for measuring UV light absorption index of the desired mixtures or liquids. Absorption cells can vary for different purposes and volumes. In this work absorption cells were used to analyze the volumetric content of the mixture retrieved from the sampling tubes in order to measure the oil accumulated in the 2nd land after one stroke of an internal combustion engine. The absorption cells used in this thesis work had 1400µl volume and 10mm light path. Specification of the absorption cells were given in the Figure 3.7.

Material Color Code:	OS
Light Path:	10 mm
Volume:	1400 µl
Outer Dimensions:	
Height:	45 mm
Width:	12,5 mm
Depth:	12,5 mm
Inner Dimensions:	
Width:	4 mm
Base Thickness:	3,2 mm
Number of windows:	2

Figure 3.7 Absorption cells used for analysis

3.6.2. Disposable Pasteur Pipettes

In this work Pasteur pipettes were used for taking the oil-hexane mixtures from the sampling tubes. After the experiments the volume contents of the oil hexane mixture were analyzed by UV light absorption spectrometer. Due to the absorption index was much depended to the volume content of the oil hexane mixture. Therefore using disposable glass Pasteur pipettes was a good solution for taking the mixture from the sampling tube without disturbing the volume content of the oil hexane mixture.

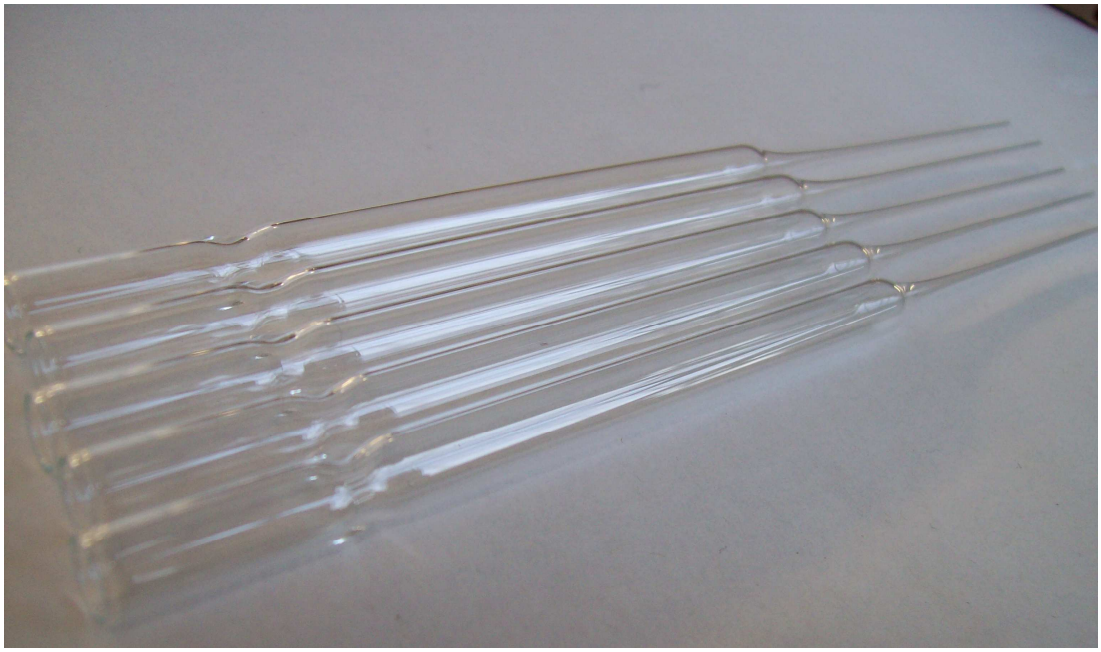

Figure 3.8 Disposable Pasteur pipettes used for analysis

CHAPTER 4

RESULTS AND DISCUSSION

In this study it was intended to study the effects of oil film thickness and temperature on the accumulation of oil in the 2nd land of internal combustion engines. The experiments were held for 5,10, 15, 30, 45, 60, 75, 90 and 105 µm oil thicknesses for oils at 30 ºC , 50 ºC, 70 ºC of oil temperature and ambient temperature which was around 14-18 ºC during experiments.

During the experiments SAE 10W-40 type engine oil was used as lubricating oil, which is known to be widely used for internal combustion engines. Table 4.1 shows mechanical properties of SAE 10W-40 oil type. Oils used in present work and İçöz's work were both multigrade (multiviscosity) oils. In SAE 10W-40 acronym, "10W" indicates that the oil meets SAE (Society Automobile Engineers) specification at -18 °C, whereas "40" indicates that the oil meets the SAE specification at 100 °C.

During the samples were retrieved through sampling tubes at approximately 5.2-5.5 bar (absolute) pressure.

Generally two sets of experiments were performed for each oil film thicknesses for different temperatures. The content analyses of the samples were performed by UV light absorption spectrophotometer. In the analysis part the volumetric ratio between oil and hexane was measured by a UV light absorption spectrophotometer device. The results found for the volumetric ratio were compared with the results of calibration curve, which was generated using known oil and hexane volumes.

Table 4.1 Properties of SAE 10W-40 engine oil

Engine oil SAE 10W-40				
Mineral based multigrade gasoline engine oil				
Property	Value in metric unit		Value in US unit	
Density at 60°F (15.6°C)	0.872 *10³	kg/m³	54.4	lb/ft³
Kinematic viscosity at 104°F (40°C)/100°F (38°C)	108.5	cSt	556	SSU
Kinematic viscosity at 212°F (100°C)/210°F (99°C)	15.4	cSt	81.5	SSU
Viscosity index	149		149	
CCS viscosity at -13°F (-25°C)	6270	cP	6270	cP
Flash point	220	°C	430	°F
Pour Point	-33	°C	-30	°F
Sulfated ash	0.86	%	0.86	%
Neutralization No. (TBN-E)	7.1		7.1	
Color	2		2	

4.1. UV Light absorption Measurements

4.1.1. Determination of Optimum Wavelength for Measurements

In order to have accurate results it was a need to work in the wavelengths where UV absorption of the oil- hexane mixture was maximum. For this purpose UV light absorption of hexane was investigated between the wavelengths of 190 nm and 700 nm for different volume fractions of oil hexane mixture shown in Table 4.2.

Table 4.2 Oil and hexane volumes used for determination of the working wavelength

	Oil Volume (µl)	Hexane Volume (ml)	Volume Ratio
Mixture 1	10	10	0.001
Mixture 2	5	10	0.0005
Mixture 3	2.5	10	0.00025
Mixture 4	1.25	10	0.000125

Investigation of the optimum wavelength for the specific mixture (oil hexane) is important in order to detect small changes in the volume fractions. After the investigation between 190 nm and 700 nm of wavelengths it was seen that UV absorption of oil hexane mixture was suitable for the measurements which would be

held at wavelength of 283 nm. As a sample, a zoomed graph of the above mentioned work is given in Figure 4.1. Results of determining the optimum wavelength are given in Appendix-D.

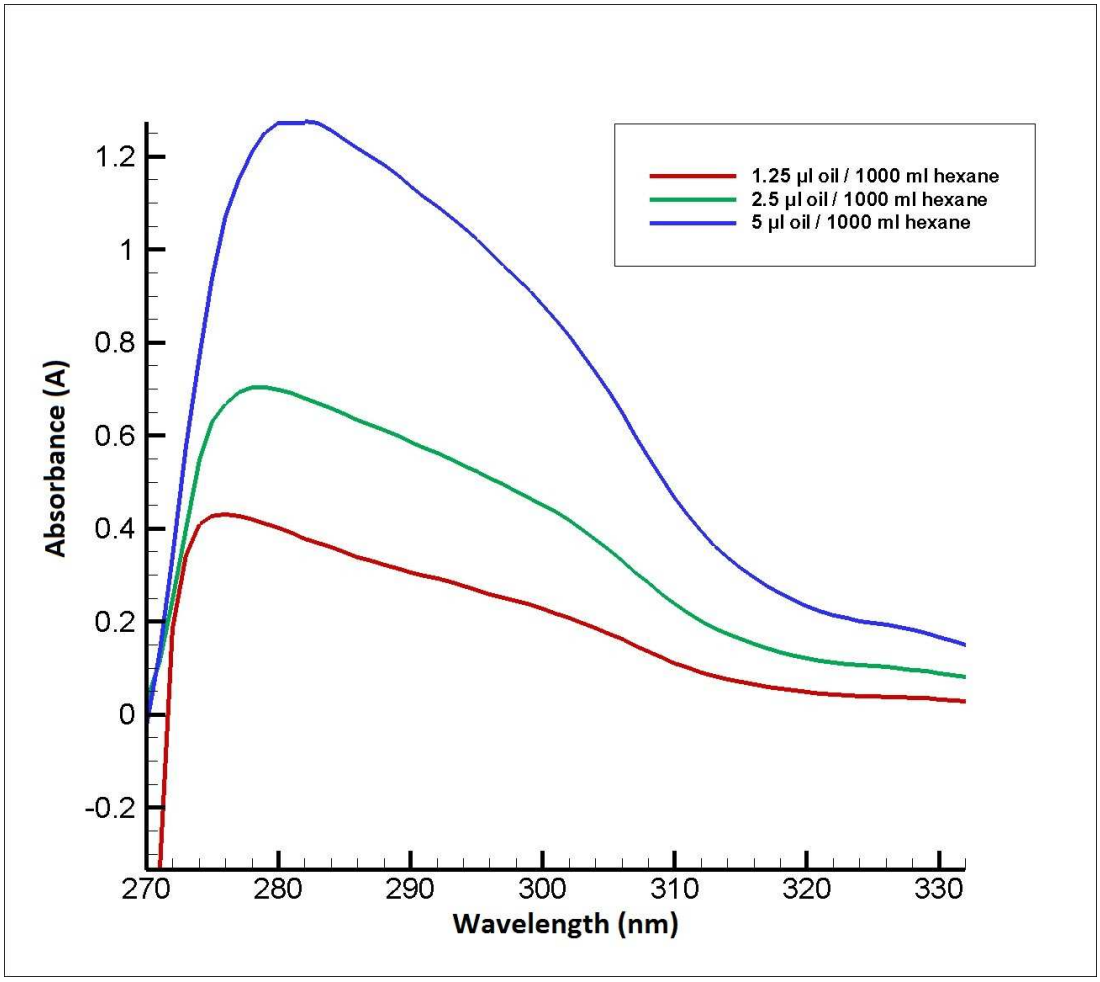

Figure 4.1 Absorption index of selected oil-hexane mixtures

4.1.2. UV Calibration Curve

Analyses of the mixture sampled from the experiments were investigated at the laboratory of Food Engineering Department. The UV light absorption was measured for every sample in order to find the volume ratio in the samples. Specifications of the UV light absorption spectrophotometer are given in Appendix-D.

With UV light absorption analysis, light absorption index of the mixture was measured. In order to match the light absorption index with the volume ratio of the mixture; light absorption indices of oil hexane mixtures of predefined volume ratios were measured and a calibration curve was found. The generation process of the calibration curve was repeated three times in order to overcome experimental inaccuracies. Results were obtained for volumetric ratios of oil hexane mixtures shown in Table 4.3.

Table 4.3 Oil and hexane volumes used for formation of the calibration curve

Oil Volume (µl)	Hexane Volume (ml)	Volume Ratio
10	10	0.001
5	10	0.0005
2.5	10	0.00025
1.25	10	0.000125

Formation of calibration curve was initiated with preparing a mixture with 10 µl oil and 10 ml (10×10^6 µl) hexane. 1500 µl from the mixture was taken in an absorption cell with the help of the pipette. After UV absorption index of the mixture was measured and recorded, 5 ml of the remaining mixture was taken in another volume and 5 ml of hexane was added into this mixture to dilute the mixture to half concentration. This procedure was repeated four times until reaching the volume ratio of 1.25×10^{-4}. The results and average values obtained from three calibration curves are plotted in Figure 4.2 with the trend line.

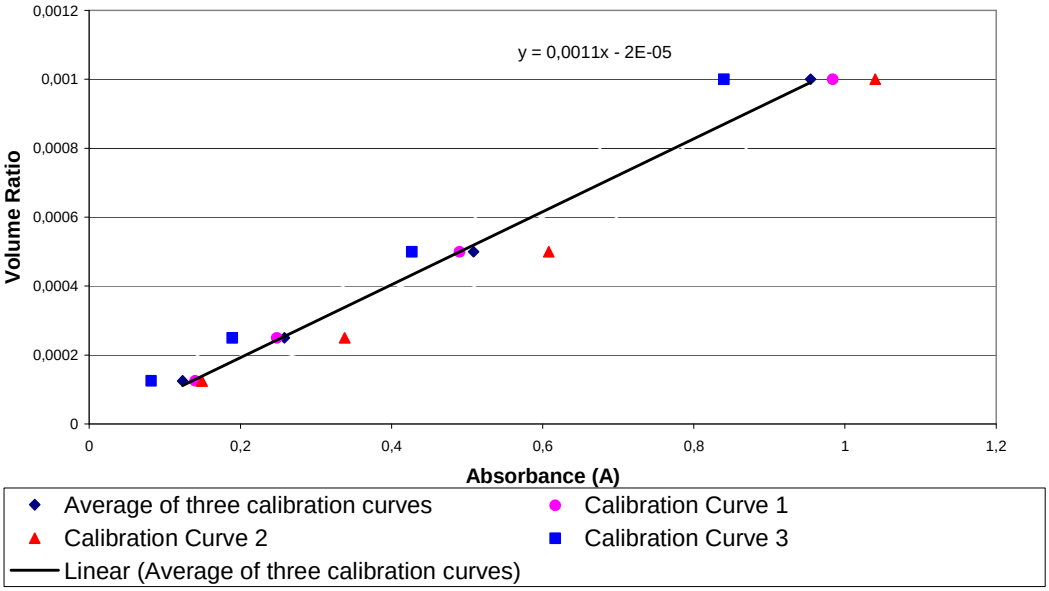

Figure 4.2 Averaged calibration curve

4.2. Accumulated Oil in the 2nd Land

4.2.1. Accumulated Oil in the 2nd Land at Ambient Temperature

The results of oil accumulated in the 2nd land are initially compared with the results obtained by İçöz [13]. İçöz used SAE 15W-30 type oil in his study in order to investigate the effects of oil film thickness on the accumulation of oil in the 2nd land. Properties of SAE 15W-30 type of oil are given in Table 4.4.

Table 4.4 Properties of SAE 15W-30 engine oil

Typical Characteristics

Characteristic	Method	Units	Typical Value
Viscosity Grade	SAE	Engine Gear	15W-30 80W-85
Density @ 15.6C	IP160	g/cm^3	0.87
Viscosity at 100°C	ASTM D445	cSt	9.4
Viscosity at 40°C	ASTM D445	cSt	65
Viscosity Index	ASTM D2270		124
Pour Point	ASTM D97	°C	-35
Sulphated Ash	ASTM D84	%wt	1.4

4.2.1.1. Accumulated Oil in the 2nd Land at 15 °C Temperature

Experiments for the oil at 15 °C temperature of oil were performed without using the heater. At least two sets of experiments were done for oil film thicknesses of 15, 30, 45, 60, 75, 90 and 105 µm.

Results of first set of experiments for oil film at ambient temperature of 15 °C are given in Figure 4.3.

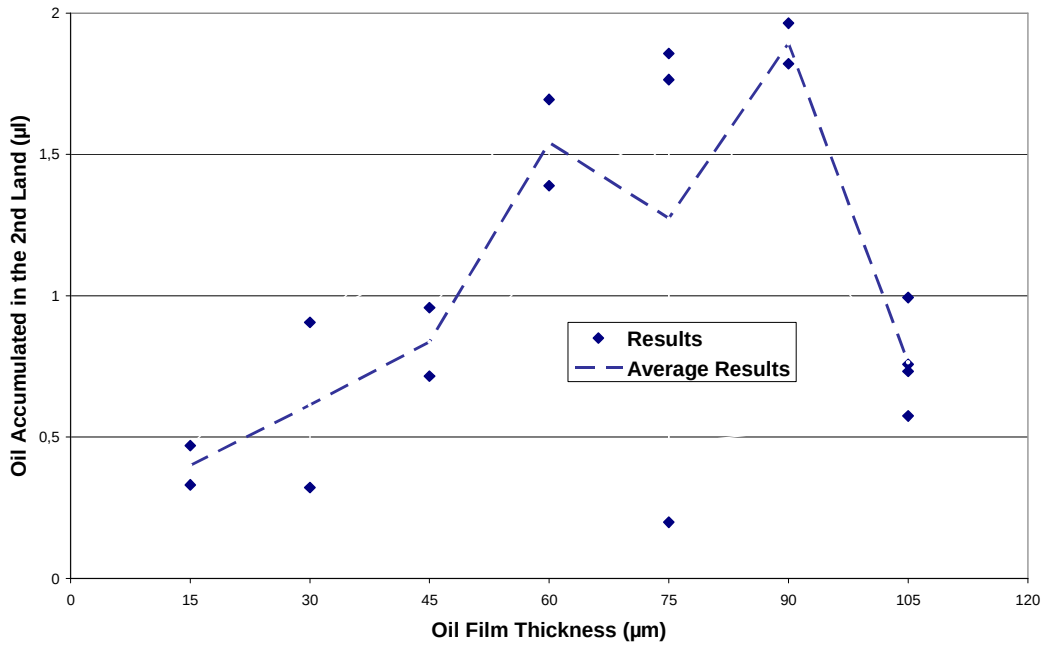

Figure 4.3 Oil accumulated in the 2nd land at 15 ℃

At 75µm oil film thickness after the second experiment of the experiment set, the difference between two results was high. This was probably due to the loss of sealing property of the sampling tube used in the experiment. The second experiment of the 75µm oil film thickness set was repeated.

At 105µm oil film thickness, both results of oil accumulated in the 2nd land were low compared to the results of experiments of other film thicknesses. Two more experiments were performed for the 105µm oil film thickness. The results obtained for the accumulated oil in the 2nd land for 105 µm oil were very close to each other.

4.2.1.2. Accumulated Oil in the 2nd Land at 18 °C Temperature

After performing experiments of oil at 30 °C, 50 °C and 70 °C it was seen that the trend of oil accumulated in the second land of results of experiments for oil at 15 °C, was not similar with the results of experiments performed for oil film at 30 °C, 50 °C and 70 °C. Comparison of the results of experiments performed at 15 °C and 18 °C oil temperature with İçöz's work [13] is given in Figure 4.5. It was evaluated that the contradiction could be due to operator error therefore it was decided to perform experiments for ambient temperature.

New experiment set of oil film at ambient temperature were performed 4 months later for oil film at 18 °C. Results of experiments for oil film at 18 °C are given in Figure 4.4.

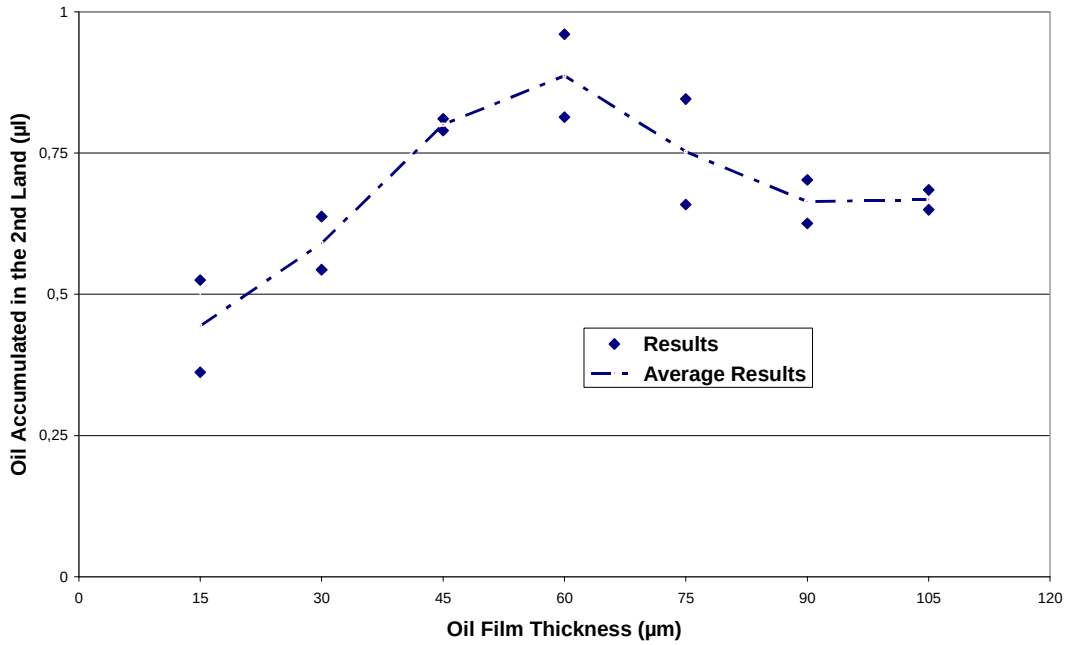

Figure 4.4 Oil accumulated in the 2nd land at 18 ℃

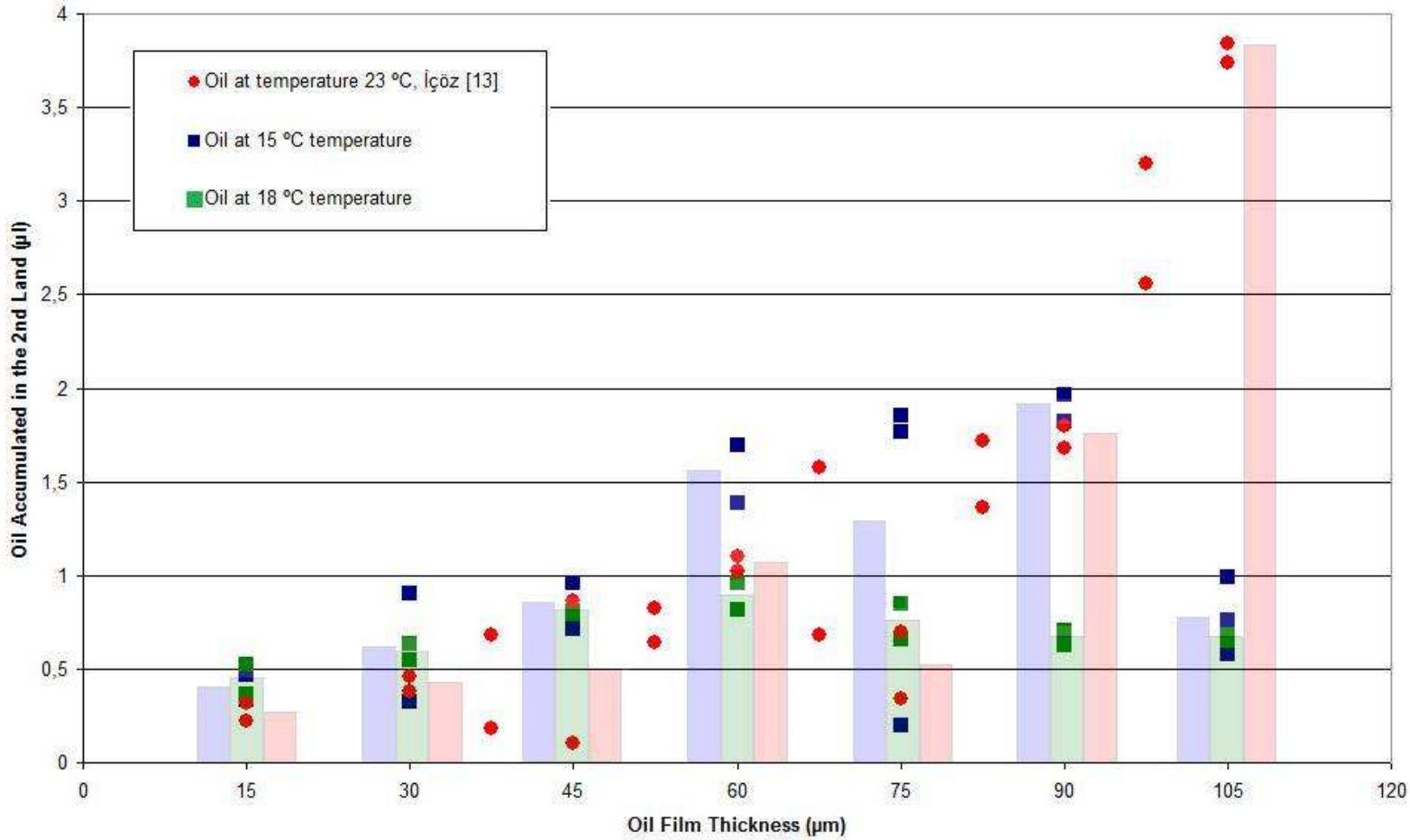

Figure 4.5 Comparison of experimental results for oil accumulated in the 2nd land at 15 °C, 18 °C and 23 °C

According to the results of the experiments for oil at 18 °C, an increase in the amount of oil accumulated in the 2nd land up to oil film thickness of 60 µm was observed. After oil film thicknesses larger than 60 µm, increasing trend of the amount of oil accumulated in the 2nd land vanished and stayed steady.

After the experiments held for 105 µm oil film thickness, during the disassembling phase for the next experiment it was noticed that the oil film near the SC over on the bottom plate surface was very thin as seen from the Figure 4.6 which is a photograph taken after the experiment.

Figure 4.6 Oil distribution on the bottom plate after the experiment

In Figure 4.6 the formation of the oil puddle around the ring end gap can be seen as stated in “The Puddle Theory of Oil Consumption” [21]. The area on the bottom

plate's surface, where thinner oil film thickness present was just below the passage demonstrating the ring end gap on the second plate.

4.2.2. Accumulated Oil in the 2nd Land at 30 ºC Temperature

Experiments for oil temperature of 30 ºC were carried out for oil thicknesses of 10, 15, 30, 45, 60, 75, 90 and 105 µm. For this temperature it was not possible to form a uniform oil film for thicknesses below 10 µm. In these experiments it was aimed to investigate the effects of temperature difference of oil on the oil accumulation in the 2nd land. High oil temperature also made it possible to investigate the oil accumulation in the 2nd land for the oil thicknesses below 15 µm.

Results of the experiments of 30 ºC of oil temperature are plotted in Figure 4.7.

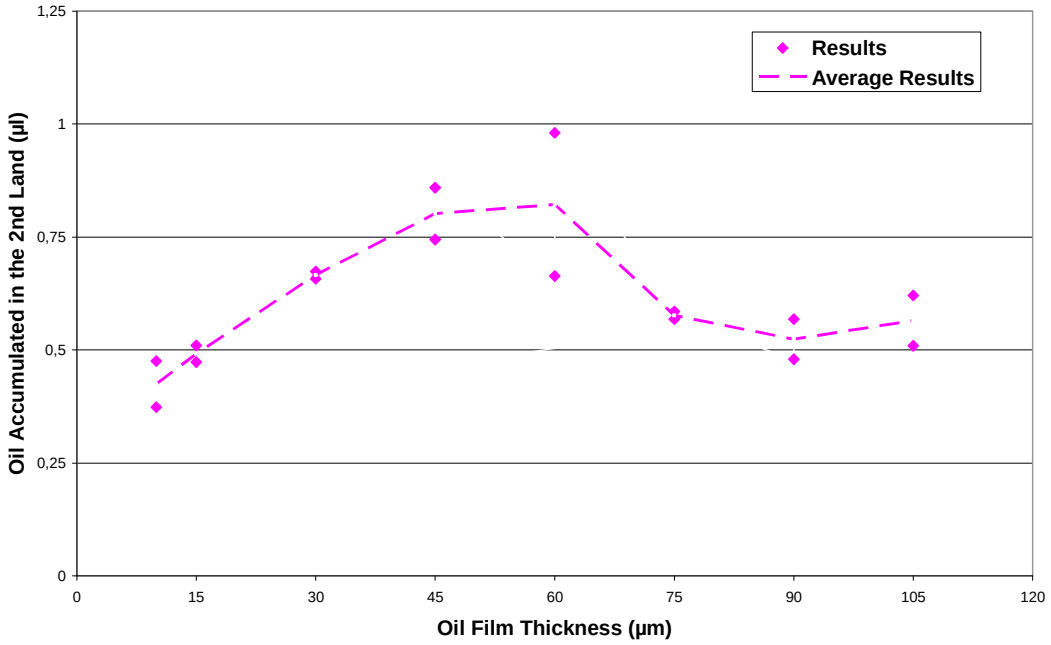

Figure 4.7 Oil accumulated in the 2nd land at 30ºC

It is seen that, the results of the experiments for oil film thicknesses larger than 60 µm, increasing trend of the amount of oil accumulated in the 2nd land vanished and stayed steady.

4.2.3. Accumulated Oil in the 2nd Land at 50 ºC Temperature

Experiments for oil temperature of 50 ºC carried out for oil thicknesses of 5, 10, 15, 30, 45, 60, 75, 90 and 105 µm. In these experiments it was aimed to investigate the effects of temperature difference of oil on the oil accumulation in the 2nd land. Experiments for high oil temperature also made it possible to investigate the oil accumulation in the 2nd land for the oil thicknesses below 15 µm.

Results of the experiments of 50 ºC of oil temperature are plotted in Figure 4.8.

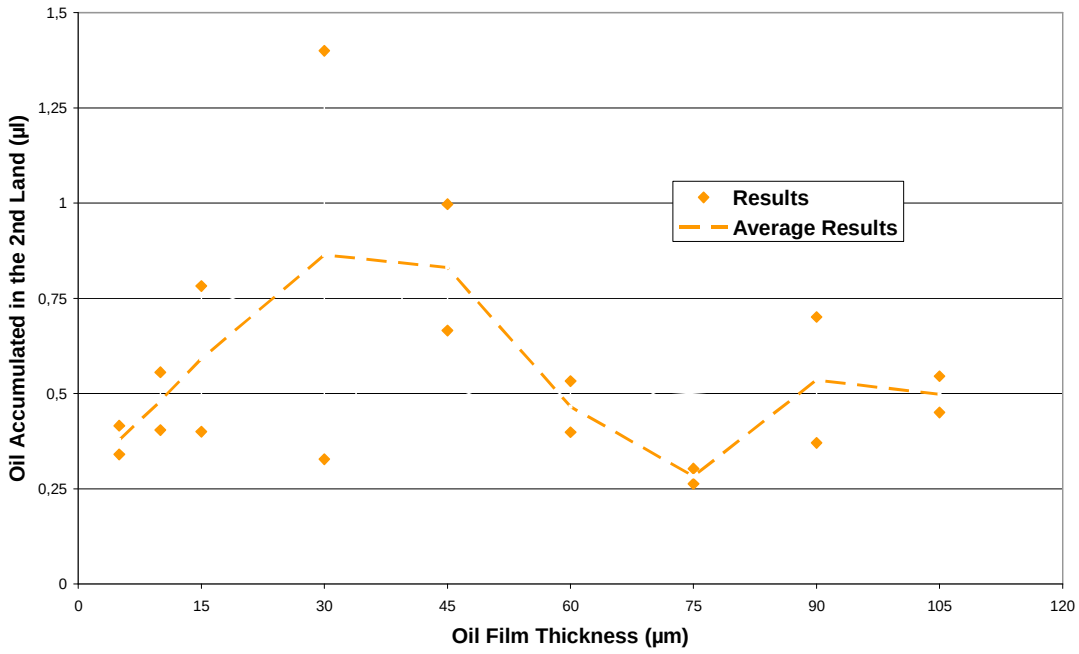

Figure 4.8 Oil accumulated in the 2nd land at 50ºC temperature

It is also seen that above 45µm oil film thickness, the amount of oil accumulated in the SC is small compared to the results of the experiments for ambient oil

temperature are below 45µm. This can be due to same phenomena with the 105µm oil film thickness experiments done at ambient temperature and the oil film thicknesses experiments done above 60 µm at 30 °C oil temperature.

It was noticed that after the experiment the oil spread on the surface of the bottom plate was very thin around the flow passage area near the SC as seen in Figure 4.9. This behavior was observed for 75 µm and 105 µm experiments for the oil at 50 ºC temperature. Some droplets near the o-ring pf the bottom plate were also observed after the 105 µm experiments of oil at 50 ºC.

Figure 4.9 Oil distribution on the surface of bottom plate

4.2.4. Accumulated Oil in the 2nd Land at 70 ºC Temperature

Experiments for oil temperature of 70 ºC were held for oil thicknesses of 5, 10, 15, 30, 45, 60, 75, 90 and 105 µm. In these experiments it was aimed to investigate the

effects of temperature difference of oil on the oil accumulation in the 2nd land. Experiments for high oil temperature also made it possible to investigate the oil accumulation in the 2nd land for the oil thicknesses below 15 µm.

Results of the experiments of 70 ºC of oil temperature are plotted in Figure 4.10.

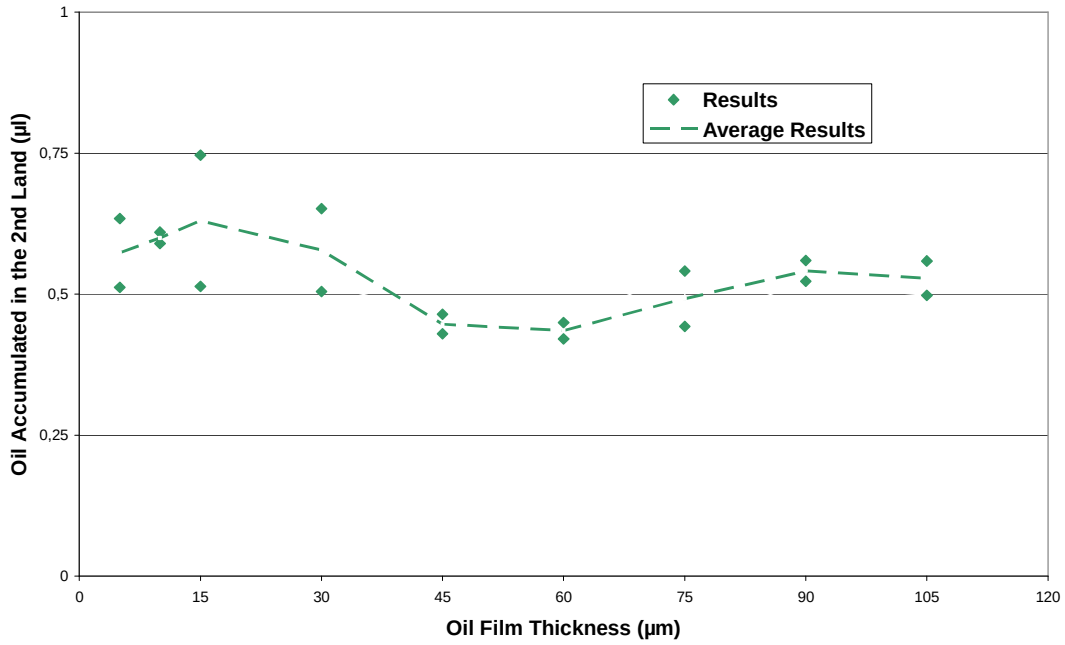

Figure 4.10 Oil accumulated in the 2nd land at 70ºC

According to the results of the experiments carried out for oil at 70 °C , it was seen that there was no big difference in the amount of oil accumulated in the 2nd land. However, up to 30 µm oil film thickness an increase in the amount of oil accumulated can be seen. After 30 µm oil film thickness the decrease in the accumulated oil is observed likewise in the experiments held for different oil temperatures. In Figure 4.11 the oil on the surface of the bottom plate after experiment held for 75 µm oil film thickness and 70 °C of oil temperature. In Figure 4.11 the formation of the oil puddle can be seen. This time the formation of the puddle was not regular as the ones observed during the experiments for other temperatures. This can be attributed to the fact that, the piston cylinder subassembly

could be disassembled approximately 15-20 minutes after the experiments due to the time needed for the assembly to cool down.

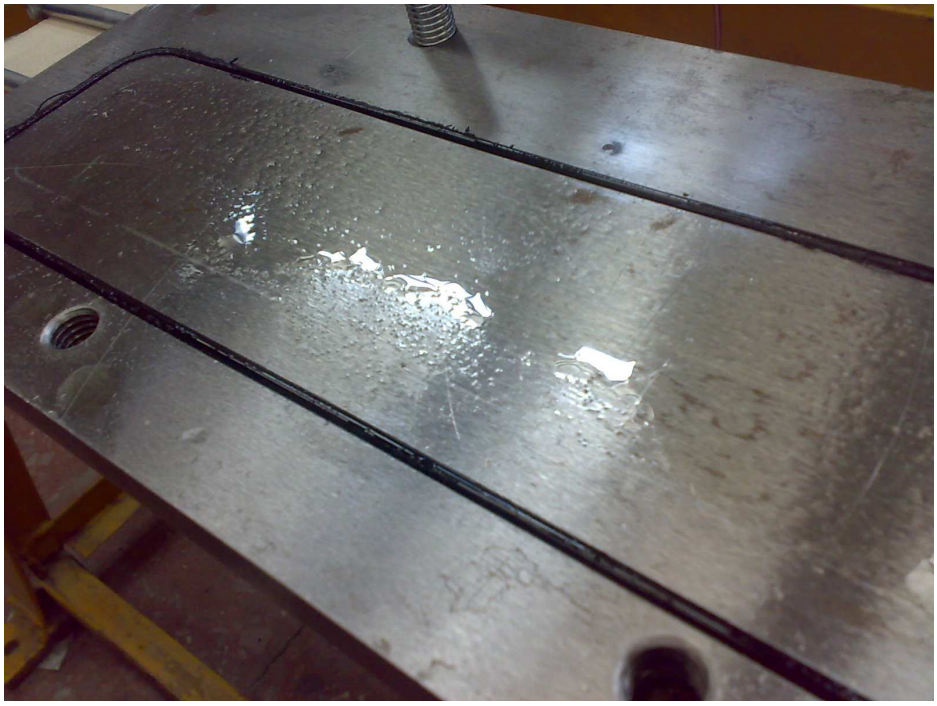

Figure 4.11 Oil distribution on the surface of bottom plate

4.2.5. Comparison of the Results for 18, 30, 50 ºC and 70 ºC Temperature

Comparison of the results of the experiments for the accumulated oil in the 2nd land is given in . According to the results of experiments; an increase in the amount of oil accumulated in the 2nd land was observed starting from the lowest oil film thickness value up to some different values of oil film thicknesses for each temperature groups. The oil film thickness values were given in Table 4. 5.

According to “The Puddle Theory of Oil Consumption” the amount of oil accumulated in the 2nd land is related to the gas velocity through the ring end gap, Taylor number of lubricating oil and geometry of the compression ring and crevice

volume. For each experiment for different temperature it was meaningful to state that Pressure difference between the combustion chamber and 2nd land and geometry were constant. As a result each, experiment should be under the conditions of approximately same gas flow profile. The stop of increase in the amount of oil accumulated in the 2nd land could be due to the change in the regime of forming droplets. For each temperature it there may be a change in the regime of forming droplets, which was shown in Figure 1.9, after peak oil film thickness point.

Table 4. 5 Oil film thickness values after decrease in the amount of oil accumulated in the 2nd land was observed

	Oil film thickness (μm)
Ambient Temperature	60
30 °C Temperature	60
50 °C Temperature	30
70 °C Temperature	15

After the experiments held for higher oil film thickness values, it was possible to see the formation of the oil puddle on the surface of the bottom plate as seen in Figure 4.6, Figure 4.9 and Figure 4.11. The oil puddle had a well shape for the experiments done at ambient temperature. For the experiments of higher temperature values the shape of the puddle was irregular. The irregular puddle shape could be due to decrease of viscosity and surface tension with increasing temperature.

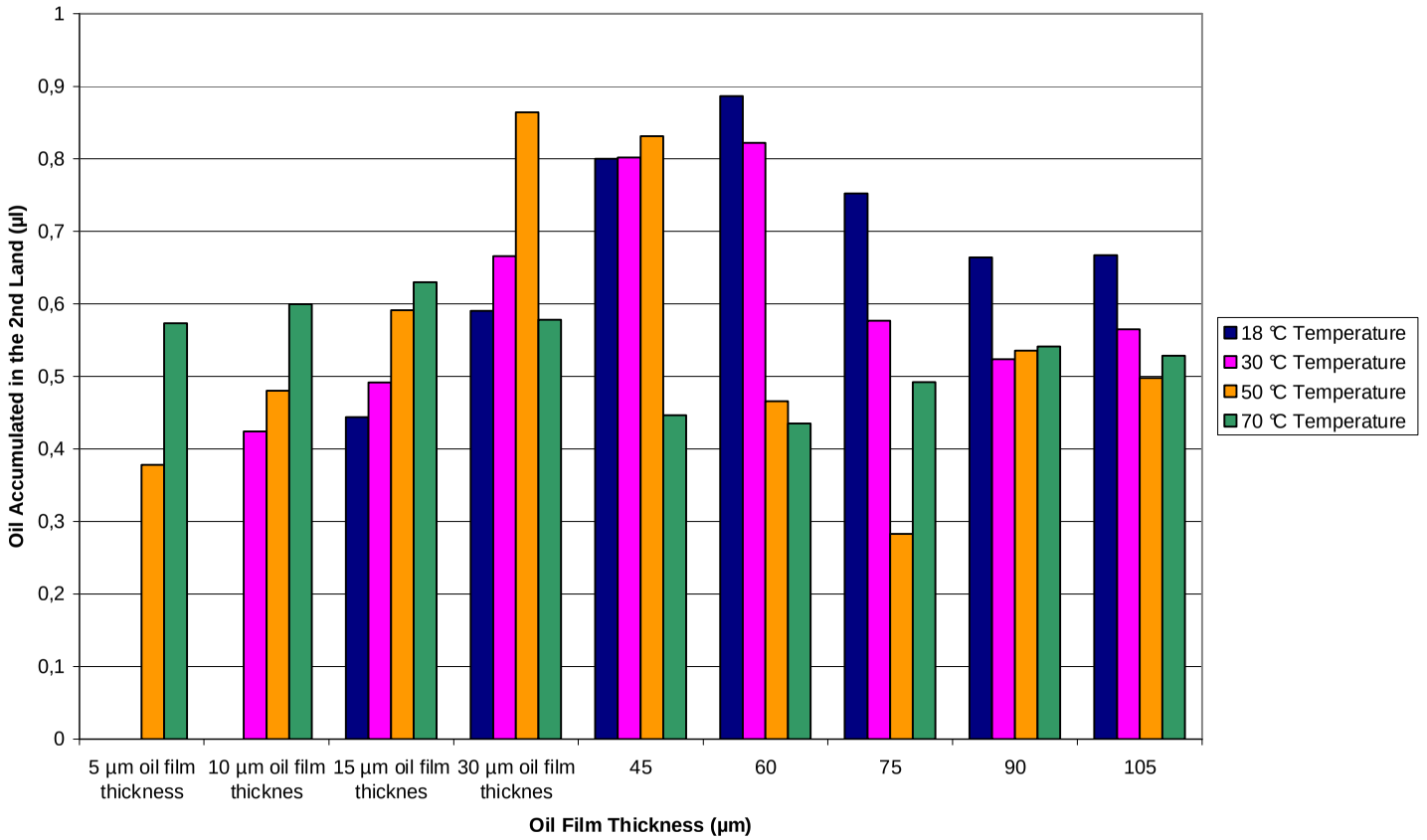

Figure 4.12 Comparison of the average experimental results for oil accumulated in the 2nd land projected oil consumption results

Oil consumption of a running diesel engine at 3000 – 4500 rpm was found to be 2 to 12 g/hr for a single cylinder [3, 10, 11 and 23]. The results found after experiments were µl oil for a single stroke (1 rpm) per cylinder. In order to compare the results with previous studies; these values were converted to grams per hour per cylinder by using conversion factors. In Figure 4.13 projected results were compared to oil losses of previous works done on operating engines.

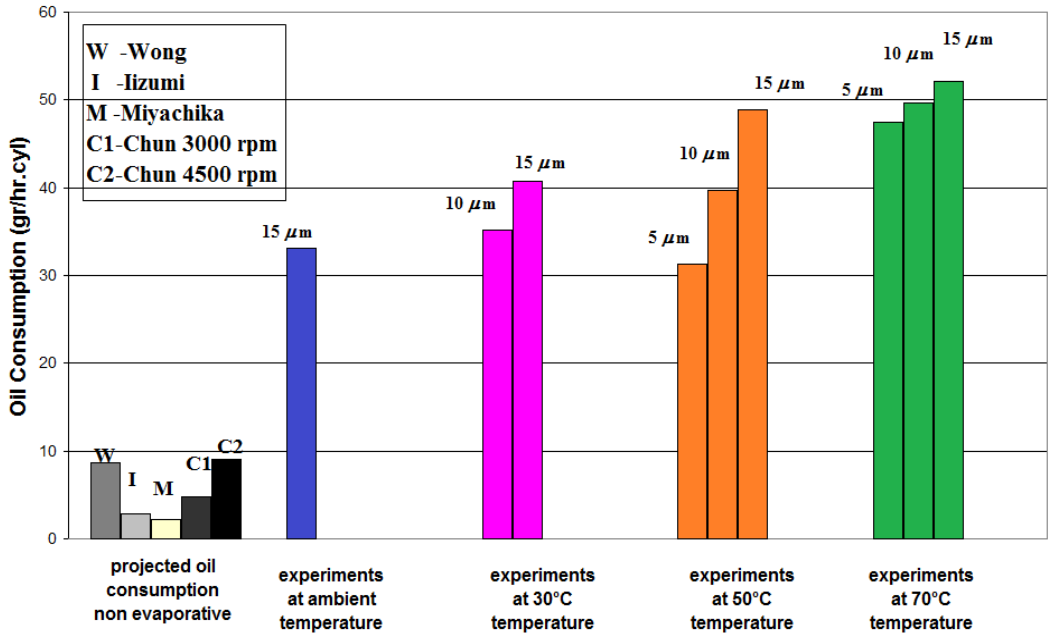

Figure 4.13 Projected oil consumption

Experimental results of oil consumption were 3-15 times larger than real consumption values. Since all the oil accumulated in the 2nd land did not pass into the consumption chamber therefore all the oil in the 2nd land was not consumed in real engines. Some of the entrained oil into the 2nd land remains still in the 2nd land where as some of the oil passes to 3rd land. Moreover in the experiments performed for ambient temperature, oil film thicknesses were larger compared to real engines which varied between 1-17 µm [23]. For lubricating oil at ambient temperature it

was not possible to spread the necessary amount of oil on the surface of the bottom plate below 15µm of oil film thickness.

4.3. Uncertainty Analysis

Instruments used in the work were pipettes for volume measurement, thermocouples for measuring the voltage difference due to temperature differences, UV light absorption spectrophotometer for measuring the volume content of oil in the mixture. Dominant uncertainty in this study was mainly due to volume measurement errors.

Data set of each oil film thickness at specific temperatures consisted of two measurements for oil accumulated in the 2nd land. It was not possible to measure standard deviation of the test results due to the small number of repeated measurements at the same experiment conditions. Uncertainty of this work was estimated by evaluating the highest and lowest values of the measurement results.

For UV light absorption analysis, 1500 µl of oil-hexane mixture obtained after one experiment was taken into the absorption cell. Initially 1100 µl of hexane was taken into the sampling tube in order provide the same amount of hexane in the sampling tube prior to the experiment as İçöz [13] did. The amount of oil-hexane mixture in the sampling tube was measured with an accuracy of 25 µl. After the experiments it was seen that the amount of oil-hexane mixture in the sampling tubes changed between 600 µl to 1050 µl. Oil-hexane mixture in the sampling tube was diluted to get 1500 µl of oil-hexane mixture as summarized in Table 4.6.

Table 4.6 Dilution Process prior to UV Analysis

Amount of oil-hexane mixture in the sampling tube after experiment	Dilution rate	Amount of oil-hexane mixture taken from the sampling tube	Amount of hexane added
over 750 µl	2	750	750
below 750 µl	3	500	1000

Volume measurements played an important role in formation of the calibration curves. The calibration curve used in this work was generated by averaging three repeated measurements for the same oil-hexane volume ratios. In uncertainty analysis, besides the averaged calibration curve, calibration curves those give the highest and minimum oil volumes against light absorption of oil-hexane mixture were also included in the calculations. Trend lines of the calibration curves giving the highest and lowest oil volume against UV light absorption are given in Figure 4.14.

A sample calculation of lowest and highest values of oil accumulated in the 2nd land is given in Table 4.7.

Table 4.7 Sample Calculation

Dilution ratio	Amount of oil-hexane mixture in the sampling tube	Amount of oil-hexane mixture added into absorption cell	Amount of hexane added into absorption cell	Calibration Curve	Calculated amount of oil in the 2nd land
2	800	750	750	y = 0,0011x - 2E-05	0,96
2	825	738	762	y = 0,0012x + 3E-05	1,3251
2	775	762	738	y = 0,001x - 6E-05	0,6134

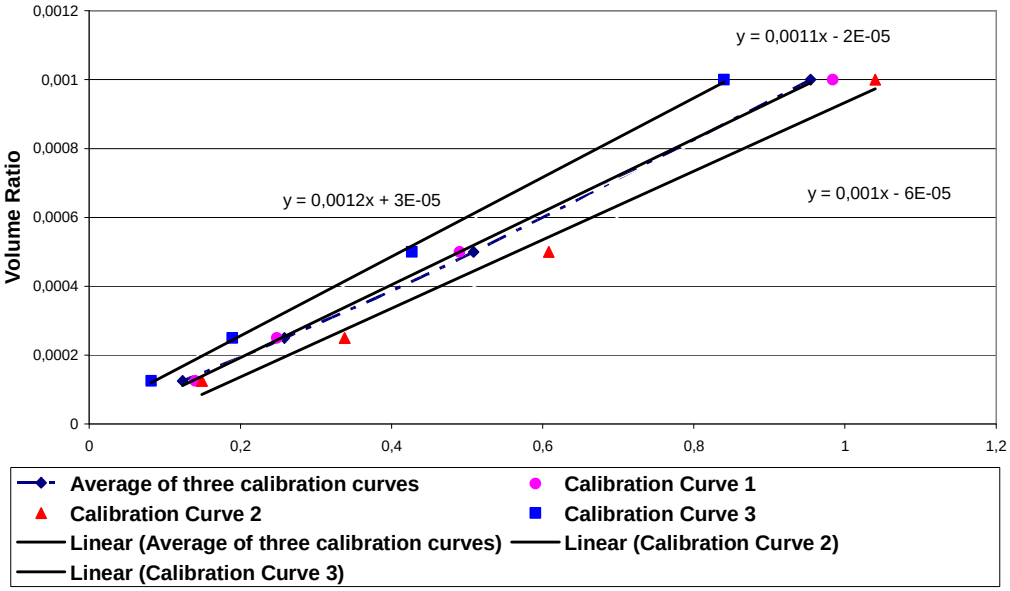

Figure 4.14 Calibration curves

According to uncertainty analysis, effects of calibration curve and volume measurement errors are summarized in Table 4.8**.**

Table 4.8 Effects of Calibration Curve and Volume Measurement Errors

Error Sources		Maximum inaccuracy (%)	Minimum inaccuracy (%)
Calibration Curve Errors	Volume Measurement Errors		
√	√	207	27
	√	4.8	2.4

As seen in Table 4.8 largest uncertainty came from differences of three calibration curves. It is evaluated that differences in calibration curves can affect the results in terms of order of magnitude of amount of oil accumulated in the 2nd land. But the results would have same trends (increase wise and decrease wise) as they are calculated by using the same calibration curve.

4.4. Future Work

In this part necessary works were evaluated in order to decrease inaccuracy in results and explain unexpected results obtained from experiments.

In part 4.3 it was stated that largest inaccuracies resulted from the differences in calibration curves. In order to lessen the inaccuracy due to calibration curve, calibration curve should be repeated enough times to end up with a curve that the repeated curves converged. Also for the experiments should be repeated more than twice in order to have a meaningful uncertainty evaluation. It was not possible to repeat the experiments more than twice for every oil film thicknesses due to lack of time.

It was stated in part 4.2.5, that the decrease in the amount of oil accumulated in the 2nd land could be due to the change in the regime of forming droplets. Two phase flow phenomenon of oil and gas was studied by Bilge [14]. In Bilge's work entrainment rate for oil was developed from Ishii and Grolmes [6] water-air flow equations as given in Equation 4.1 and Equation 4.2.

Modified Weber number:

$$We = \frac{\rho_{gas} V_{gas} D_h}{\sigma_{oil}} \left(\frac{\rho_{oil} - \rho_{gas}}{\rho_{gas}} \right)^{1/3} \quad (4.1)$$

Entrainment rate:

$$\dot{\varepsilon} = 0.935 \times 10^{-5} \zeta \exp\left(-1.87 \times 10^{-5} \zeta^2\right) \rho_{oil} V_{oil} \, \mathrm{Re}_{oil}^{0.5} \, We^{-0.25} E$$

$$+0.022 \rho_{oil} V_{oil} \, \mathrm{Re}_{oil}^{-0.26} \left(\frac{\mu_{gas}}{\mu_{oil}} \right)^{0.26} E^{0.74} \times \left(1 - \exp\left(-1.87 \times 10^{-5} \zeta^2\right)\right)^{0.74} \quad (4.2)$$

Weber number is the ratio of the inertial forces to surface tension, according to above equation; it was expected that the entrainment rate therefore amount of oil accumulated in the 2nd land is more dependent on the Reynolds number.

In Figure 4.15, we can see the pressures of the modelled combustion chamber and 2nd land. obtained by İçöz in 2001. The shaded area in Figure 4.15 represents the part of the flow occurs under sonic conditions. Entrainment rate discussed in Equation 4.2 was developed for subsonic flows. Further efforts about two phase flow of oil-air flow would be helpful to understand the change in the increasing trend of amount of oil accumulated in the 2nd land after a value of oil film thickness.

In İçöz's work an increasing trend with increasing oil film thickness was detected. It is hardly possible to conclude the contradiction between two experiment results due to use of different oils in experiments. In order to investigate the dependency of the amount of oil accumulated in the 2nd land enlarging the scope of this thesis work by repeating experiments with different oil types maybe helpful to understand the entrainment phenomenon.

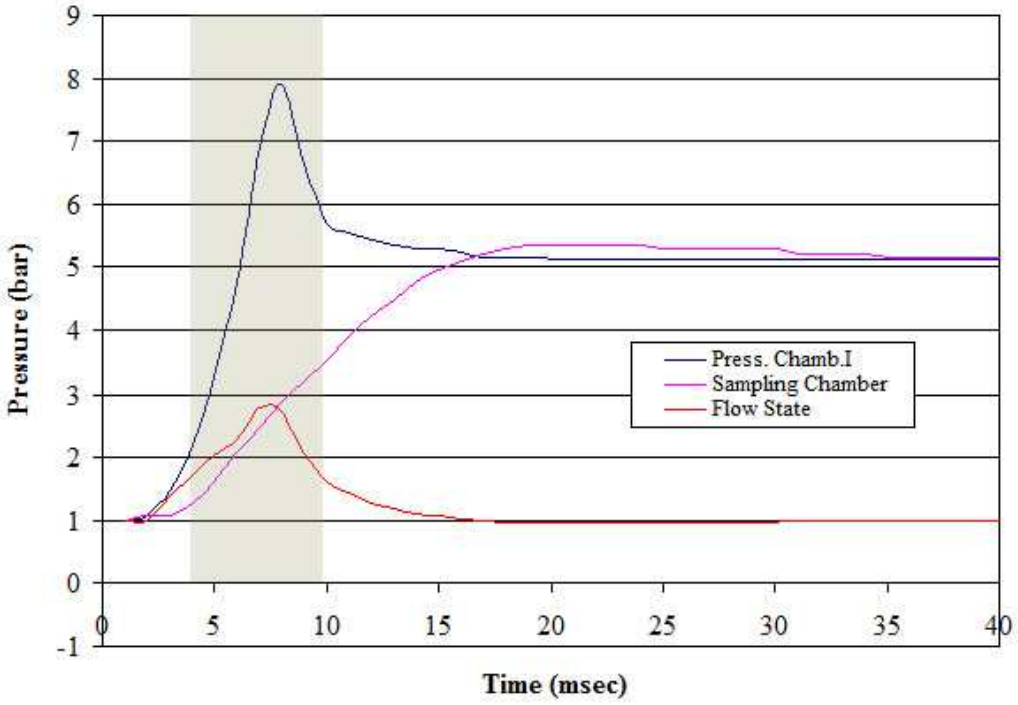

Figure 4.15 Pressure variations in modeled combustion chamber and 2nd land

In order to explore this hypothesis experiments should be repeated for different oil types.

CHAPTER 5

CONCLUSIONS

In this thesis study it was aimed to investigate the effects of the individual parameters such as oil film thickness and oil temperature on the accumulation of the oil in the 2nd land in internal combustion engines. The experimental setup used for the investigation was design and constructed as a part of a M.S. thesis by Tunç İÇÖZ, in 2001, Middle East Technical University in Mechanical Engineering Department. It was shown that the experimental setup could be utilized for investigation of the oil accumulation in the 2nd land of the internal combustion engines [13].

After the experiments performed for different oil film thicknesses at different oil temperatures following conclusions were made.

1) Amount of oil accumulated in the 2nd land crevice of internal combustion engines is affected by the oil film thickness of the oil on the cylinder wall.
2) The amount of oil accumulated in the 2nd land grows with increasing oil film thickness. But after a value of oil film thickness decrease in the amount of oil accumulated in the 2nd land was observed. The oil film thickness values, after which decrease was observed, were different for experiments held for different oil temperatures as seen in Table 4. 5.
3) The amount of oil accumulated in the 2nd land crevice of internal combustion engines is also affected by the temperature of the oil.

4) The amount of oil accumulated in the 2nd land increases with the increasing oil temperature. It was seen that below oil film thicknesses of 30 µm accumulated oil in the 2nd land increased with both increasing oil film thicknesses and oil temperature.

5) It is concluded that the amount of oil accumulated in the 2nd land can contribute oil consumption in internal combustion engines considerably.

The installation of heater to the existing experimental setup made it possible to investigate the effect of oil film thickness on the accumulation of oil in the 2nd land crevice in internal combustion engines for the oil film thickness below 15µm. This was due to the decrease of the viscosity and surface tension of the lubricating oil on the cylinder wall. It was seen that results obtained for the oil film thicknesses below 15µm was similar in the order of magnitude with oil consumption values of operating internal combustion engines.

REFERENCES

[1] Hanaoka, M., Ise, A., Nagasaka, N., Osawa, H. Arakawa, Y. and Obata, T.,1979, “New Method for Measurement of Engine Oil Consumption (S-Trace Method)”, SAE Paper No: 790936.

[2] Wahiduzzaman, S., Keribar, R., Dursunkaya, Z. and Kelley, F.A., 1992, “A Model for Evaporative Consumption of Lubricating Oil in Reciprocating Engines”, SAE Paper No: 922202.

[3] Miyachika, M., Hirota, T. and Kashiyama, K., 1984, “A Consideration on Piston Second Land Pressure and Oil Consumption of Internal Combustion Engine”, SAE Paper No: 840099.

[4] Kim, C.G., Bae, C.S. and Choi, S.M., 2000, “Importance of inter-ring crevice volume as a source of unburned hydrocarbon emissions–numerical considerations,” Journal of Automobile Engineering, vol. 214 n.4, pp. 395–403

[5] Kuo, T.W., Sellnau, M.C., Theobald, M.A. and Jones, J.D., 1989, “Calculation of Flow in the Piston-Cylinder-Ring Crevices of a Homogeneous Charge Engine and Comparison with Experiment,” SAE Paper No: 890838.

[6] Nakashima, K., Ishihara, S. and Urano, K., 1995, “Influence of Piston Ring Gaps on Lubricating Oil Flow into the Combustion Chamber,” SAE Paper No: 952546.

[7] Nakashima, K., Ishihara, S., Urano, K. and Murata, K., 1996, “Lubricating Oil Flow into the Combustion Chamber and its Reduction Method in an Automobile Gasoline Engine,” SAE Paper No: 962034.

[8] Saito, K., Igashira, T. and Nakada, M., 1989, “Analysis of Oil Consumption by Observing Oil Behaviour Around Piston Ring Using a Glass Cylinder Engine,” SAE Paper No: 892107.

[9] Hewitt, G.F. and Hall-Taylor, N.S., 1970, “Annular Two–Phase Flow,” Pergamon Press, New York, pp. 136–142.

[10] Lizumi, S. and Koyama, T., 1986, “Measurement of Oil Consumption of Diesel Engine by S-Trace Method,” SAE Paper No: 860545.

[11] Wong, V.W. and Hoult, D.P., 1991, “Experimental Survey of Lubricant Film Characteristics and Oil Consumption in a Small Diesel Engine,” SAE Paper No: 910741.

[12] Kim, C.G., Bae, C.S. and Choi, S.M., 2000, “Importance of inter-ring crevice volume as a source of unburned hydrocarbon emissions–numerical considerations,” Journal of Automobile Engineering, vol. 214 n.4, pp. 395–403

[13] İçöz, T., 2001, “Experimental Investigation of Oil Accumulation in the Inter Ring Volumes in Internal Combustion Engines”, M.S. Thesis, Department of Mechanical Engineering, METU.

[14] Bilge, E., 2009, “Computer Modeling of Blowback Oil Consumption in Internal Combustion Engines”, M.S. Thesis, Department of Mechanical Engineering, METU.

[15] Kökdemir, H.G., 1970, “Mechanical Valve Operated Shock Tube,” M.S. Thesis, Mechanical Engineering Department, Middle East Technical University, pp. 25–38, 71–73.

[16] Ishii, M., and Grolmes, M. A., 1975, ‘‘Inception Criteria for Droplet Entrainment in Two-Phase Concurrent Film Flow,’’ AIChE J., 21, pp. 308–318.

[17] Ishii, M., and Mishima, K., 1989, ‘‘Droplet Entrainment Correlation in Annular Two-Phase Flow,’’ Int. J. Heat Mass Transfer, 32, pp. 1835–1846.

[18] Hoult, David P., andShaw II, Byron T., 1994, “The Puddle Theory of Oil Consumption”, Tribology Transactions, 37: 1, 75 — 82.

[19] Green, R. M., and Cloutman, L. D., 1997, “Planar LIF observations of unburned fuel escaping the upper ring-land crevice in an SI engine,” SAE Paper No: 970823.

[20] Zenon Pawlak, 2003, “Tribochemistry of Lubricating Oils,” Tribology and Interface Engineering, pp 301-316.

[21] Roderick, M., Lusted, 1994, “Direct Observation of Oil Consumption Mechanisms In a Production Spark Ignition Engine”, MS in Mechanical Engineering, Massachusetts Institute of Technology.

[22] E., G., Giakoumis, 2008, “Lubricating oil effects on the transient performance of a turbocharged diesel engine,” Energy, Volume 35, Issue 2, pp 864-873

[23] Sang, Myung, Chun, 2005, “A Study on Engine Oil Consumption”, Journal of KSTLE, Vol., 21, No:6, pp 296-301

APPENDIX A

EXPERIMENTAL SETUP

Table A. 1 Dimensions of the modeled heavy duty diesel engine

Piston Dimensions	
Bore Diameter	125 mm
Stroke	140 mm
Number of Rings	3
1st Land Diameter	124 mm
2nd Land Diameter	124.44 mm
3rd land Diameter	124.44 mm
1st Groove Diameter	112.27 mm
2nd Groove Diameter	112.27 mm
3rd Groove Diameter	114.36 mm
Ring End Gaps	0.5 mm
1st Ring Groove Thickness	3.5 mm
2nd Ring Groove Thickness	3.2 mm
3rd Ring Groove Thickness	3.5 mm
Distance of Groove Top From The Piston Crown 1	5.7 mm
Distance of Groove Top From The Piston Crown 2	16 mm
Distance of Groove Top From The Piston Crown 3	24 mm
Ring Dimensions	
Thickness of 1st Ring	3 mm
Thickness of 2nd Ring	2.8 mm
Thickness of 3rd Ring	3.2 mm
Width of 1st Ring	5.1 mm
Width of 2nd Ring	5.1 mm
Width of 3rd Ring	3.4 mm

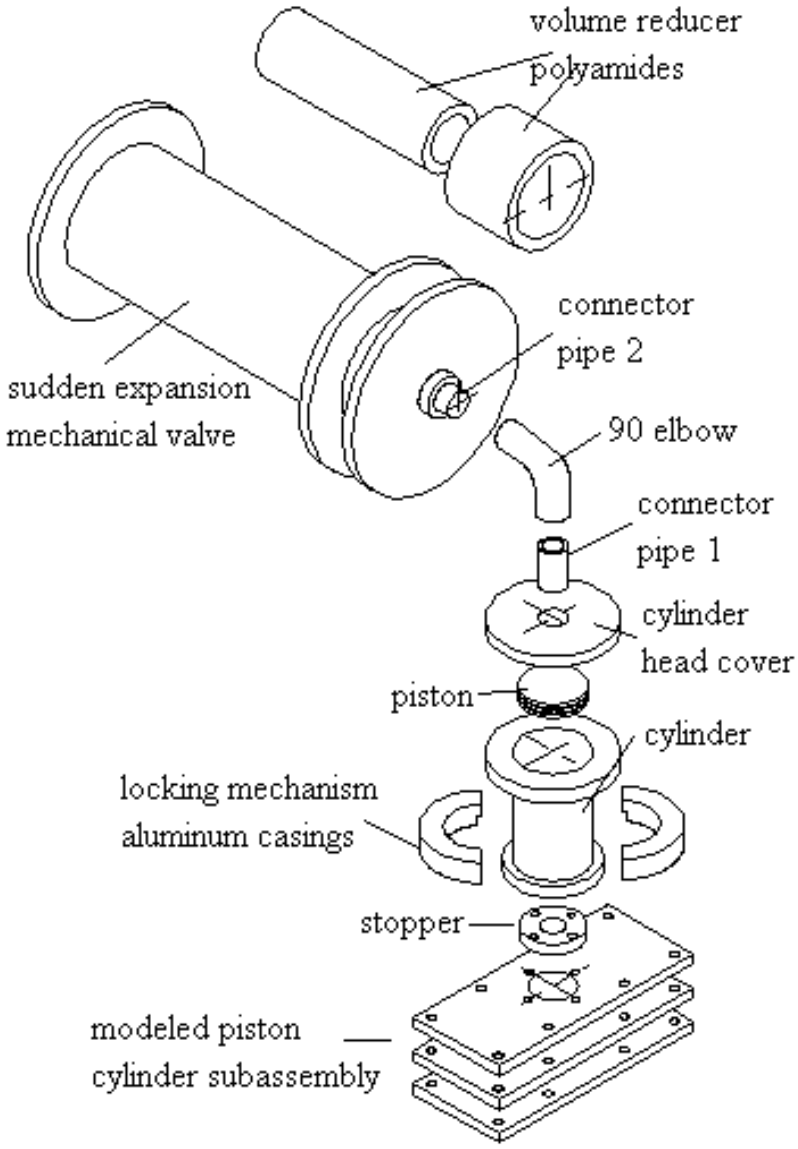

Figure A.1 Experimental setup assembly

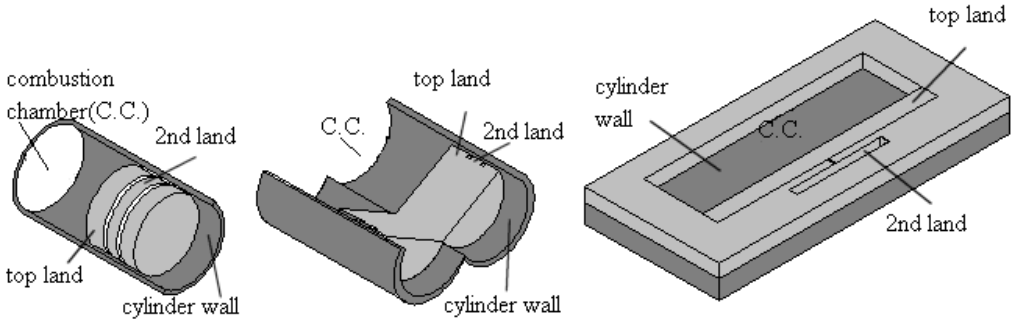

Figure A.2 Schematic representation of geometric transformation [13]

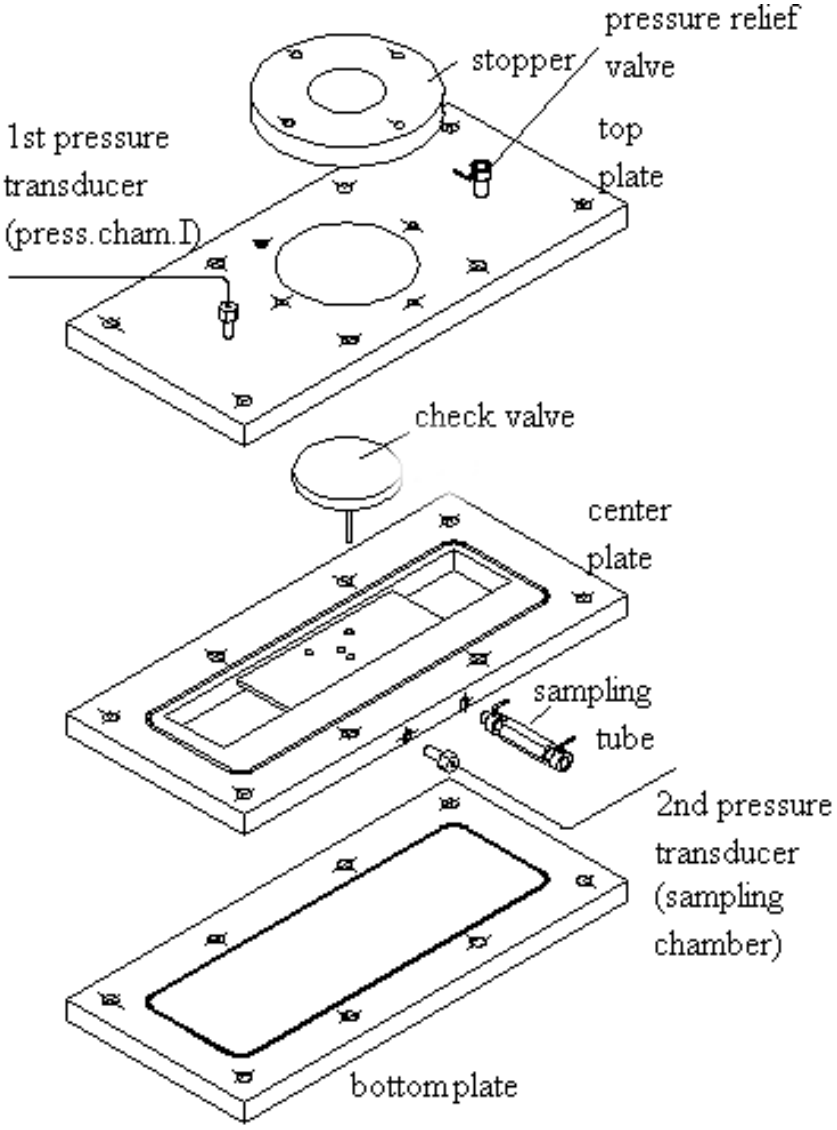

Figure A.3 Piston cylinder subassembly [13]

(a)

(b)

Figure A.4 Center plate of the modeled piston cylinder subassembly
(a) top view b) bottom view

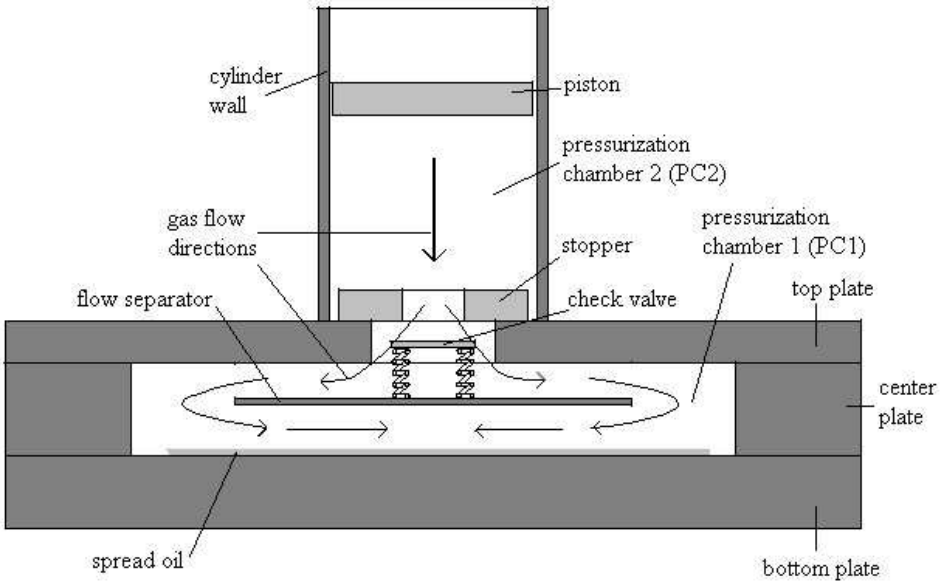

Figure A.5 Schematic representation of flow separator and flow paths

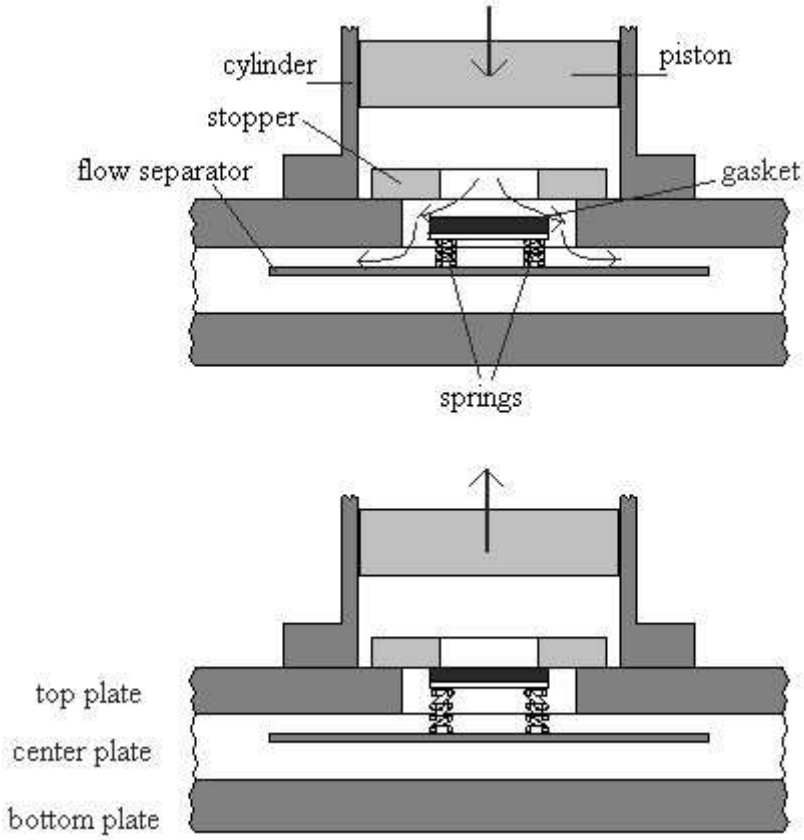

Figure A.6 Schematic illustration of check valve operation [13]

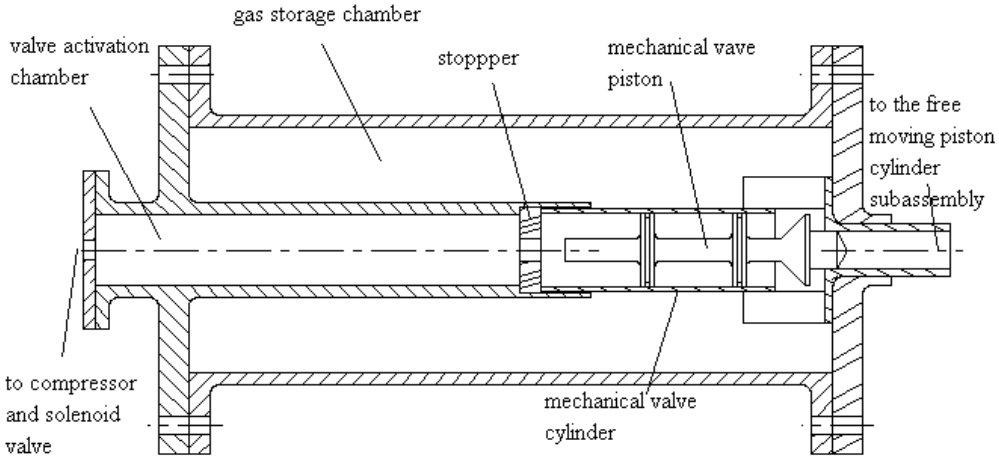

(a)

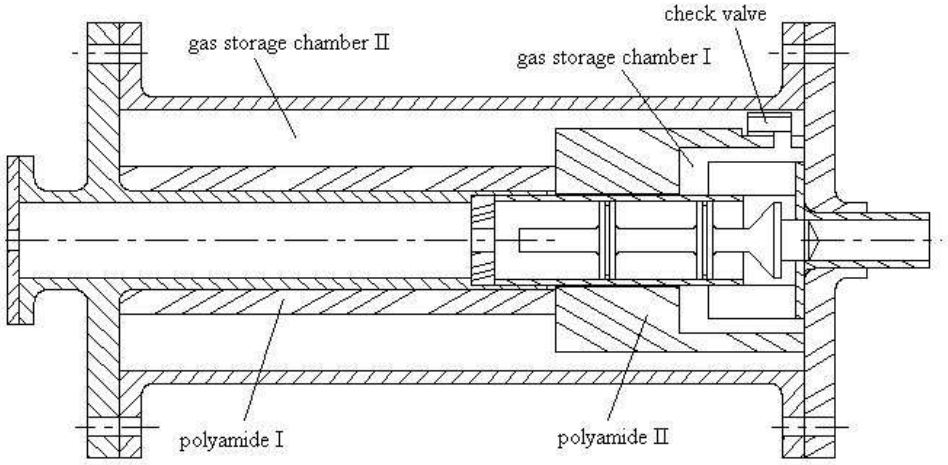

(b)

Figure A.7 Components of the sudden expansion mechanical valve (a) before and (b) after the modifications [13]

APPENDIX B

EXPERIMENTAL PROCEDURE

The experiments had been performed in the Fluid Mechanics Laboratory, the oil content analyses had been done in the Laboratory of Food Engineering Department. Required precautions should be taken prior to the experiments since the experiments have been performed at high pressures. If there occurs anything unusual, the compressor must be turned off first, and the system must be depressurized safely. The necessary maintenance must be done after all safety checks have been performed.

The experiment can be divided into three parts.

i) The preparation of the experimental setup
ii) Pressurization and sample collection
iii) The analysis of oil content in the sampling tube using UV light absorption.

The first two parts of the experiments were performed in the Fluid Mechanics Laboratory in Mechanical Engineering Department. The first part involves the assembling of the experimental setup before the experiments and is divided into two due to the usage of the heater in the experiments. The second part involves the activation of the sudden expansion of the mechanical valve and pressurization of the piston cylinder subassembly. After the piston cylinder subassembly pressurized the air sweeps the spread oil on the surface of the bottom plate, and oil is entrained into the air and flows into the SC and then sampling tube. Hexane is added prior to the experiments. As the piston stops, the oil entrained by the gas flow passes to the SC.

By opening the sampling tube a portion of the oil mist in the SC passes through the sampling tube and dissolves in hexane. The third step involves the analysis of the oil content in the sampled mixture by means of UV light absorption spectrometer.

In the assembly of the setup, the stopper was mounted to the top plate and was not disassembled between experiments again. Similarly, the cylinder was connected to the top plate and was not disassembled between experiments again. The polyamides in the mechanical valve were not removed in any of the experiments. The cylinder head cover was connected to the 90° elbow, which was also mounted to the exit of the mechanical valve.

B.1 Preparation of the Experimental Setup for the Experiments of Ambient Temperature

Step by step preparation of the experimental setup was as follows;

1) Spread engine oil in predefined thickness to the top surface of the bottom plate of the modeled piston cylinder assembly.
2) Place the bottom o-ring, and put the center plate on top of the bottom plate.
3) Locate the check valve springs and circular plate on the center plate.
4) Place the center o-ring, and put the top plate and stopper on top of the bottom plate.
5) Assemble the modeled piston cylinder subassembly.
6) Place the piston into the cylinder.
7) Slide the modeled piston cylinder subassembly and cylinder together under the cylinder head cover.
8) Connect the cylinder head cover and gasket to the cylinder.
9) Turn on the compressor.
10) Connect the solenoid valve to the electricity.

11) Add 1.1ml n-hexane into the sampling tube and connect it to the modeled piston cylinder assembly.

    (n-hexane acts as a solvent for engine oil and all the oil inside dissolves. So oil would be separated from air. Since n-hexane is highly volatile this process must be done in a well ventilated area)

12) Check that all the nuts and studs are sufficiently tightened.

After a visual inspection of the possible missing details, the experimental setup would be ready for the experiments.

B.2 Preparation of the Experimental Setup for the Experiments of Higher Temperatures

The step by step preparation of the experimental setup for desired temperatures was as follows;

1) Prepare the ice-water mixture for the 0 ºC reference for thermocouples, then insert the tip of the reference of thermocouples.
2) Place the heater on the support leg.
3) Raise the support in order to make the heater to touch with the bottom surface of the bottom plate.
4) Plug in the power cable of the adjustable voltage supplier and bring the switch to the 80 V.
5) Wait until the bottom plate was heated to the desired temperature.
6) Spread engine oil in predefined thickness to the top surface of the bottom plate of the modeled piston cylinder assembly.
7) Unplug the power cable of the adjustable voltage supplier.
8) Place the bottom o-ring, and put the center plate on top of the bottom plate.

9) Locate the check valve springs and circular plate on the center plate.
10) Place the center o-ring, and put the top plate and stopper on top of the bottom plate.
11) Assemble the modeled piston cylinder subassembly.
12) Place the piston into the cylinder.
13) Slide the modeled piston cylinder subassembly and cylinder together under the cylinder head cover.
14) Connect the cylinder head cover and gasket to the cylinder.
15) Locate the heater on the support provide the necessary contact with the bottom plate.
16) Plug in the power cable of the voltage supplier of heater and bring to 80 V.
17) Wait until the thermocouples shows the desired temperature.
18) Unplug the heater.
19) Turn on the compressor.
20) Connect the solenoid valve to the electricity.
21) Add 1.1ml n-hexane into the sampling tube and connect it to the modeled piston cylinder assembly.

(n-hexane acts as a solvent for engine oil and all the oil inside dissolves. So oil would be separated from air. Since n-hexane is highly volatile this process must be done in a well ventilated area)

22) Check that all the nuts and studs are sufficiently tightened.

After a visual inspection of the possible missing details, the experimental setup would be ready for the experiments.

B.3 Pressurization and Sample Collection

The experimentation requires high attention since high pressures exist on the setup. The valve configuration and corresponding numbering for the air connection line is shown in Figure B.1. The experimentation procedure is as follows;

1) Before opening valve 1, open valve 2 to prevent initial pressure build up inside the connection line.
2) Open valve 1 until the air from the compressor begins to flow.
3) Open valve 3 and close valve 2 in order to partially pressurize the activation chamber. This would close the mechanical valve automatically.
4) Open valve 4 to pressurize the gas storage chambers I and II.
5) Close valves 3 and 4 when both pressure gauges show 9 kg/cm^2 .
6) Close valve 1 and open valve 2 to release the pressure inside the connection line.
7) Start running the data acquisition software.
8) Switch on the solenoid valve, which will activate the experimental setup.

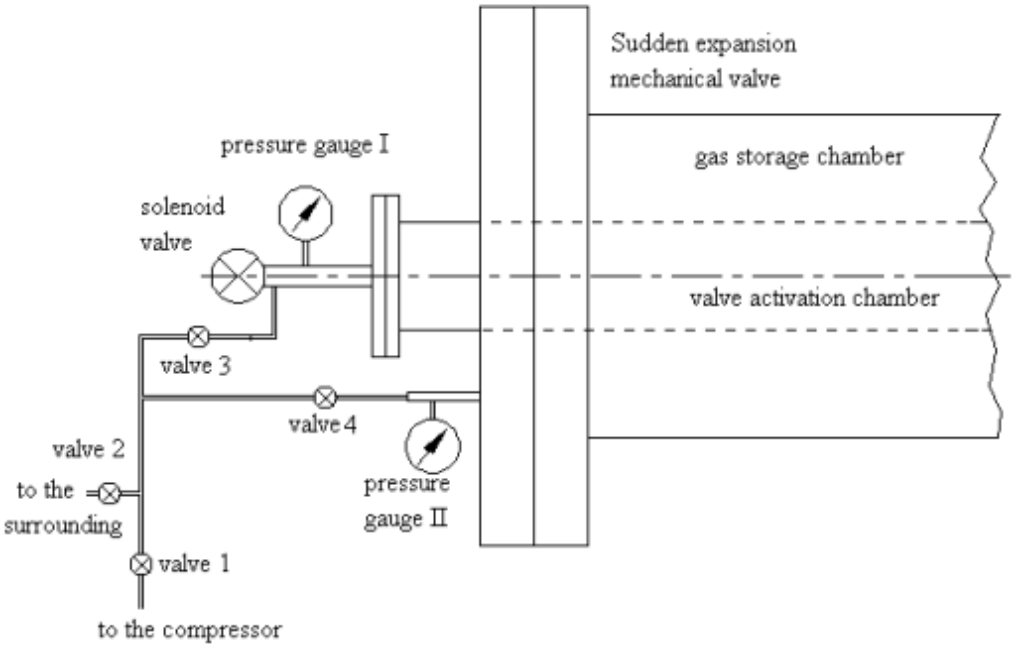

Figure B.1 The valve configuration and numbering for the air connection line

(Note that the data acquisition software will automatically stop running after 2 seconds. So the solenoid valve must be activated within 2 seconds after the software is started running)

9) When the system stabilizes (piston stops) open the valve of the sampling tube then close.
10) Open the pressure relief valve on PC1.
11) Open valves 4 to depressurize GSC1.
12) Disconnect the sampling tube from the setup.
13) Shake the sampling tube so that n-hexane inside dissolves the oil in the mixture.
14) After waiting 30 minutes, depressurize the sampling tube slowly that no liquid n-hexane escapes.

B.4 Oil Content Analysis Using UV Light Absorption Spectrometer

The analysis phase of the experiments was carried out in Food Engineering Laboratory. This stage involves the analysis of the oil content of the sampled mixture by UV light absorption spectrometer. After retrieving the oil mist in hexane by the help of sampling tube, sampling tubes were taken to the Food Engineering Laboratory and the following procedure is followed for the analysis.

1) Turn on the UV light spectrometer.
2) Set the wavelength of the UV light absorption spectrometer to 283 nm.
3) By using a pipette with a clean tip, add 750µl hexane into the absorption cell in order to clean it prior to the analysis. After emptying the cell make the cell wait for at least 30 second.
4) Add 1500µl hexane to the cell and measure the blank UV absorption value. By using “auto zero” button on the UC light absorption spectrometer set the measured UV as zero reference. After this process empty the cell again.
5) Open the sampling tube slowly. By using a disposable Pasteur pipette take all the mixture into an eppendorf tube and close.
6) Add 750µl hexane into another eppendorf tube and close.
7) By using a pipette take 750µl from the mixture and add into the eppendorf which had 750µl hexane in it. Now the mixture in the sampling tube was diluted by ½.
8) Take 1500µl of the new oil hexane mixture and put into the absorption cell.
9) Put the cell in the UV light absorption spectrometer and measure the light absorption value of the mixture.

The wavelength of the UV light absorption spectrometer must be adjusted to wavelength where the absorption was maximum or at least local maximum.

APPENDIX C

STRESS ANALYSIS OF THE BOTTOM PLATE PRIOR TO MODIFICATION

In this appendix, the stress analyses prior to the modification of the bottom plate were given.

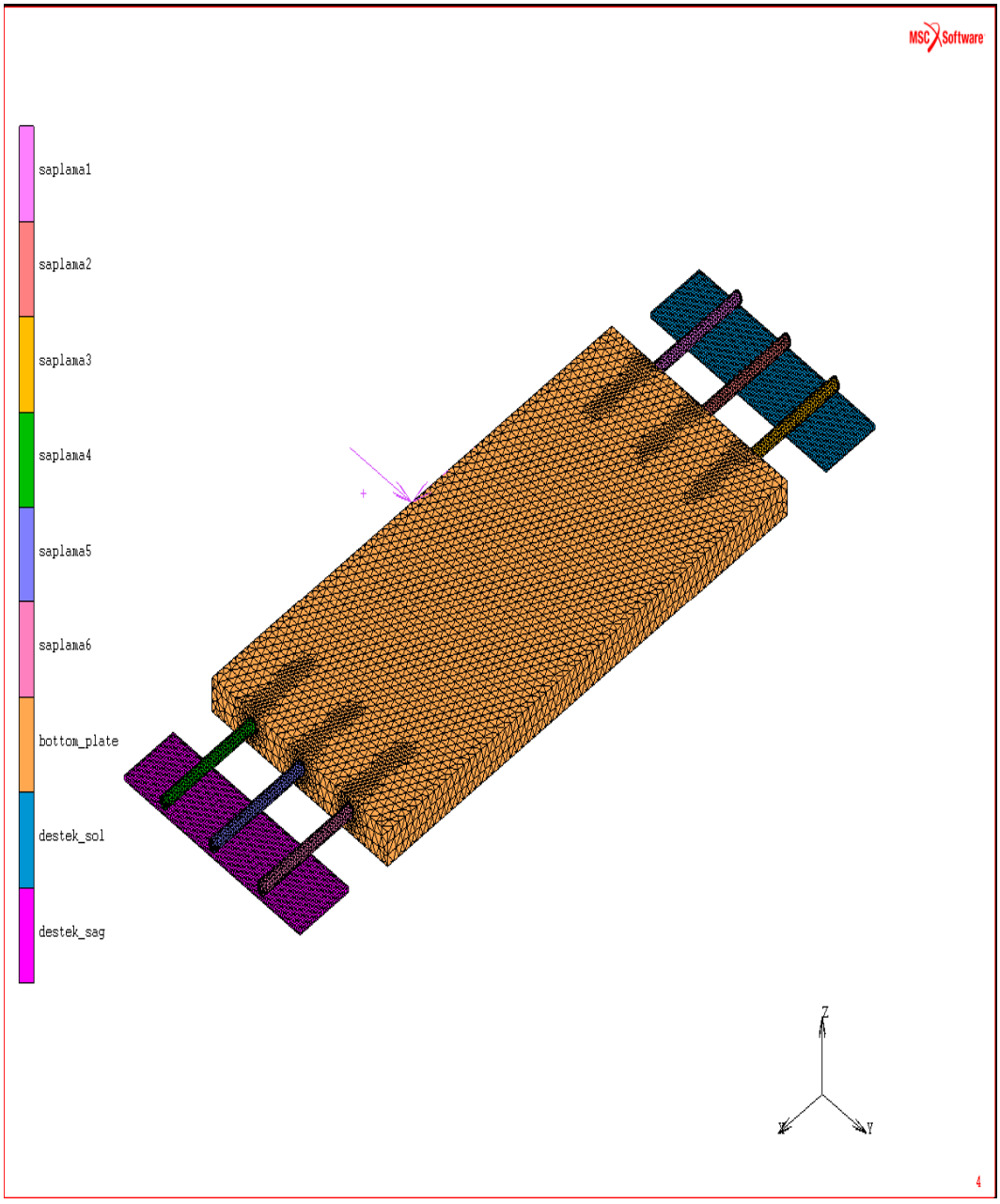

Figure C.1 Solution mesh for the studs and bottom plate

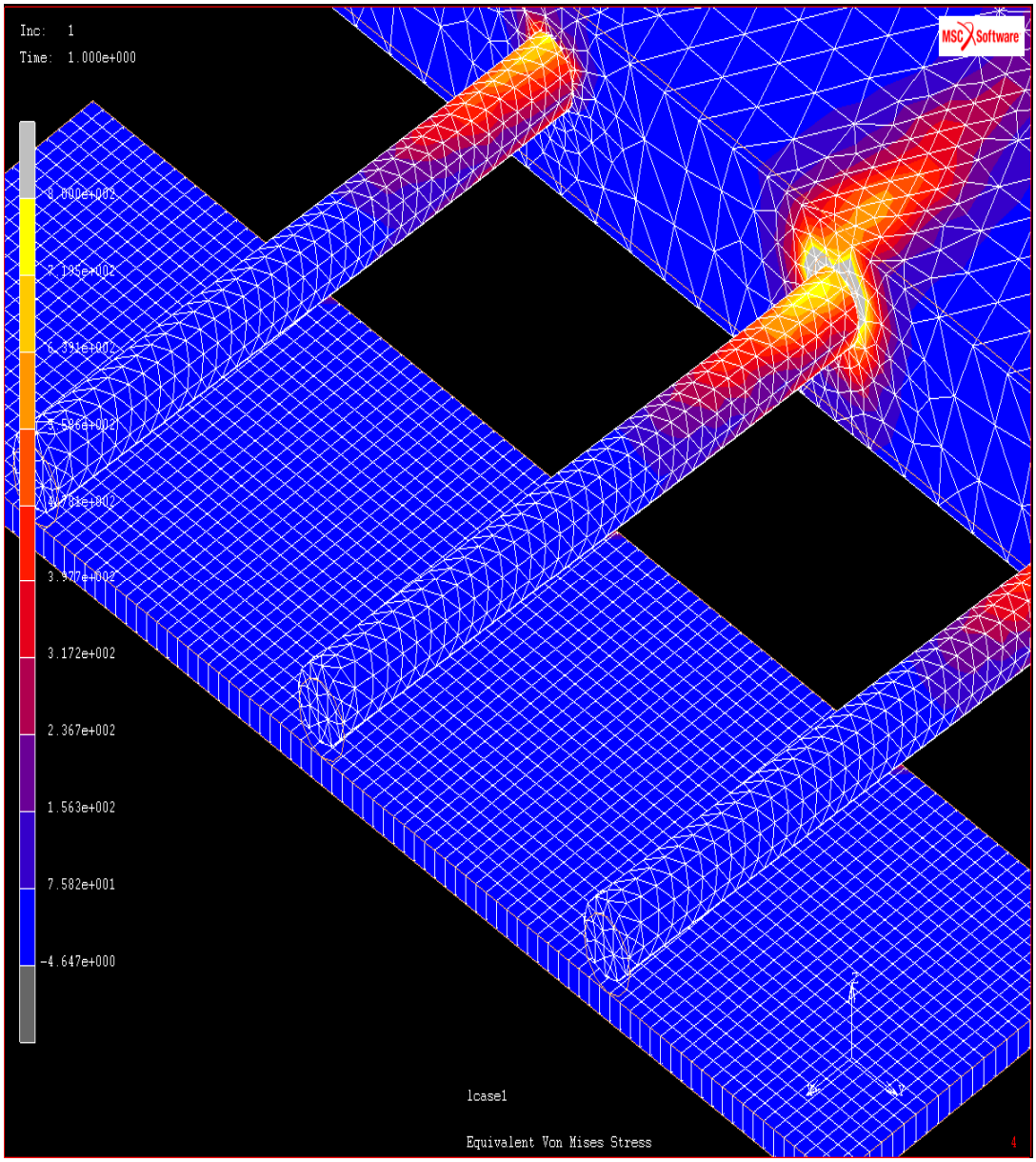

Figure C.2 Equivalent von Mises stress

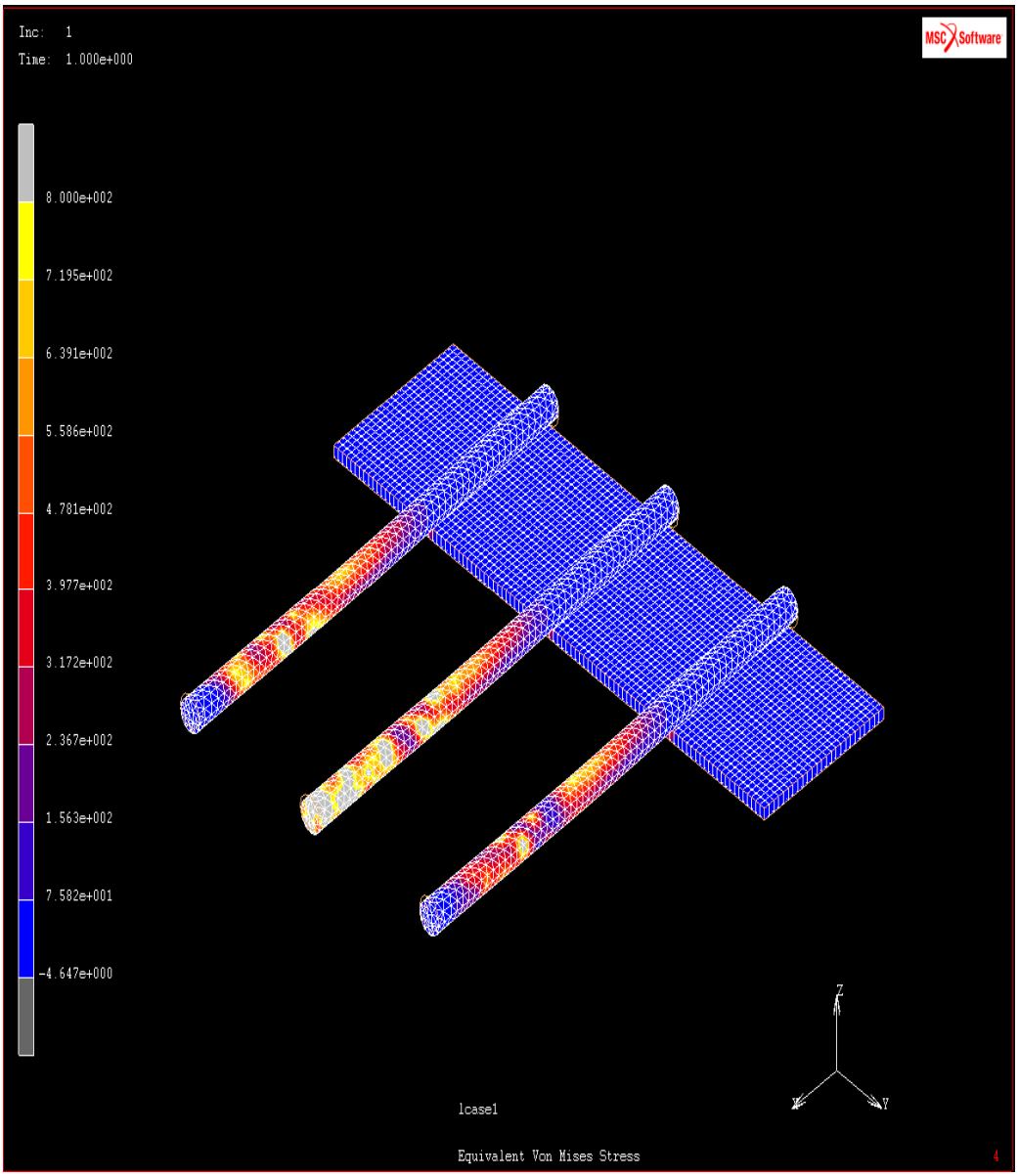

Figure C.3 Equivalent von Mises stress on the studs

APPENDIX D

D. TECHNICAL DRAWINGS OF THE MANUFACTURED PARTS

In this appendix, technical drawings of the manufactured parts are given. The technical drawings of the sudden expansion mechanical valve can be found in Kökdemir, 1970. Technical drawings of the experimental setup can be found in İçöz, 2001.

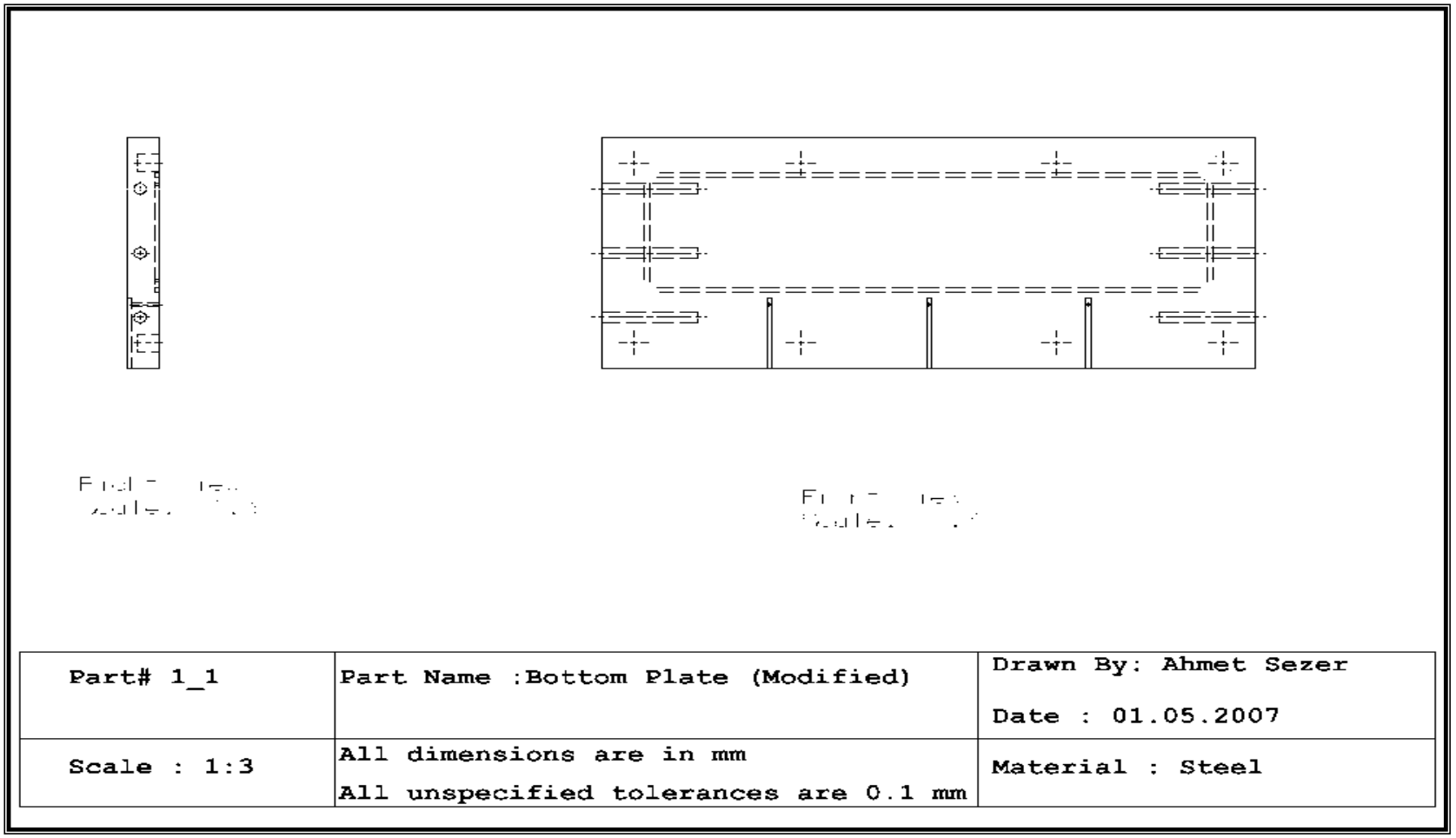

Part# 1_1	Part Name :Bottom Plate (Modified)	Drawn By: Ahmet Sezer Date : 01.05.2007
Scale : 1:3	All dimensions are in mm All unspecified tolerances are 0.1 mm	Material : Steel

Figure D.1 Technical drawings for modification of bottom plate

APPENDIX E

UV LIGHT SPECTROPHOTOMETER ANALYSIS

E.1. Determination Of The Working Wavelength For The Oil Hexane Mixture For Uv Light Absorption Analysis

Determination of the working wavelength for measuring the UV light absorption of the desired mixture was very important in order to be able to detect the volume fraction changes in terms of light absorption. Procedure of determination of working wavelength is described below.

1- Open the UV spectrophotometer and wait for machine to initialize.
2- Clean the absorption cell with hexane and let it to dry.
3- Fill the absorption cell with hexane for the baseline measurements. For the following measurements this will be the baseline for the comparison process of the oil hexane mixture. Set the limiting wavelength values for the scan process.
4- Prepare the initial oil hexane mixture for the desired volume fraction and keep it in a well sealed jar. The volume fraction of the first mixture will be mentioned as “A”.
5- Fill the absorption cell with oil hexane mixture which has the volume fraction A. Scan for the limiting wavelengths and save the graph and data.
6- Dilute the mixture A to A/2 volume fraction. Fill the absorption cell with “A/2” and scan. After scanning save the data and graph.

7- Dilute the mixture A/2 to A/4. Fill the absorption cell with “A/2” and scan. After scanning save the data and graph.
8- Dilute the mixture A/4 to A/8. Fill the absorption cell with “A/2” and scan. After scanning save the data and graph.
9- After collecting all necessary data, compare them in the same graph in order to decide the working wavelength. When deciding the working wavelength seek for the highest absorption values for all volume fractions.

E.2. Sample Results For The Optimum Working Wavelength

In this part, sample graphical results of the scan of absorption values between 190 nm and 700 nm are given.

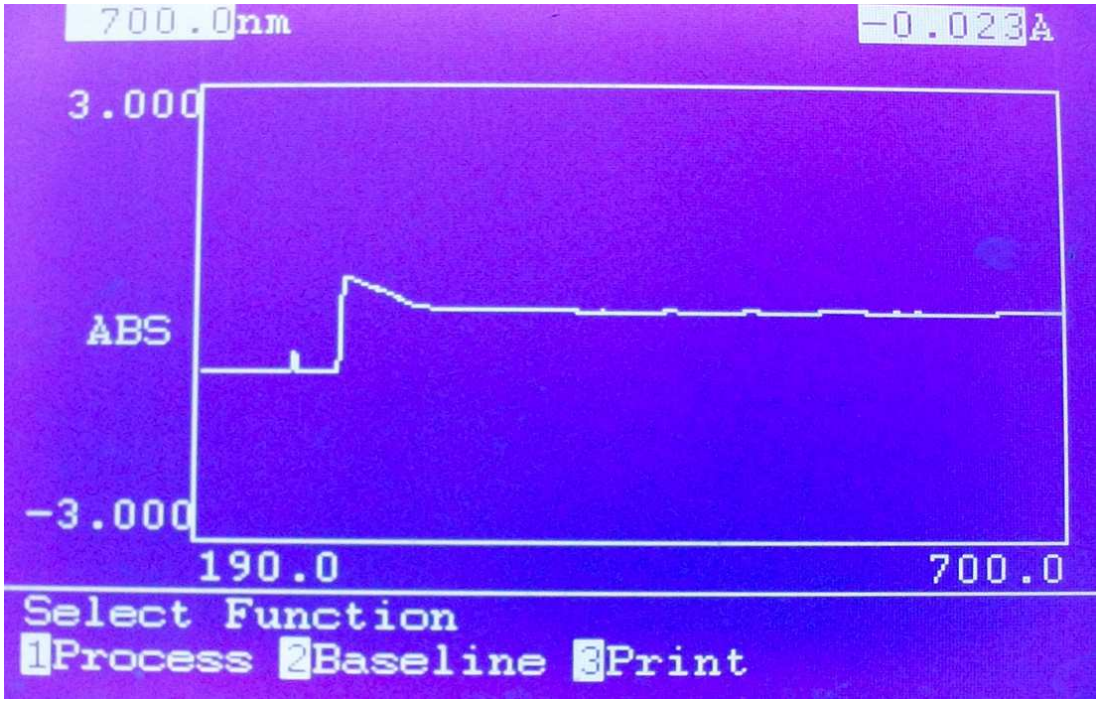

Figure E.1 Absorption of oil hexane mixture of the volume fraction A/8 between 190 nm and 700nm

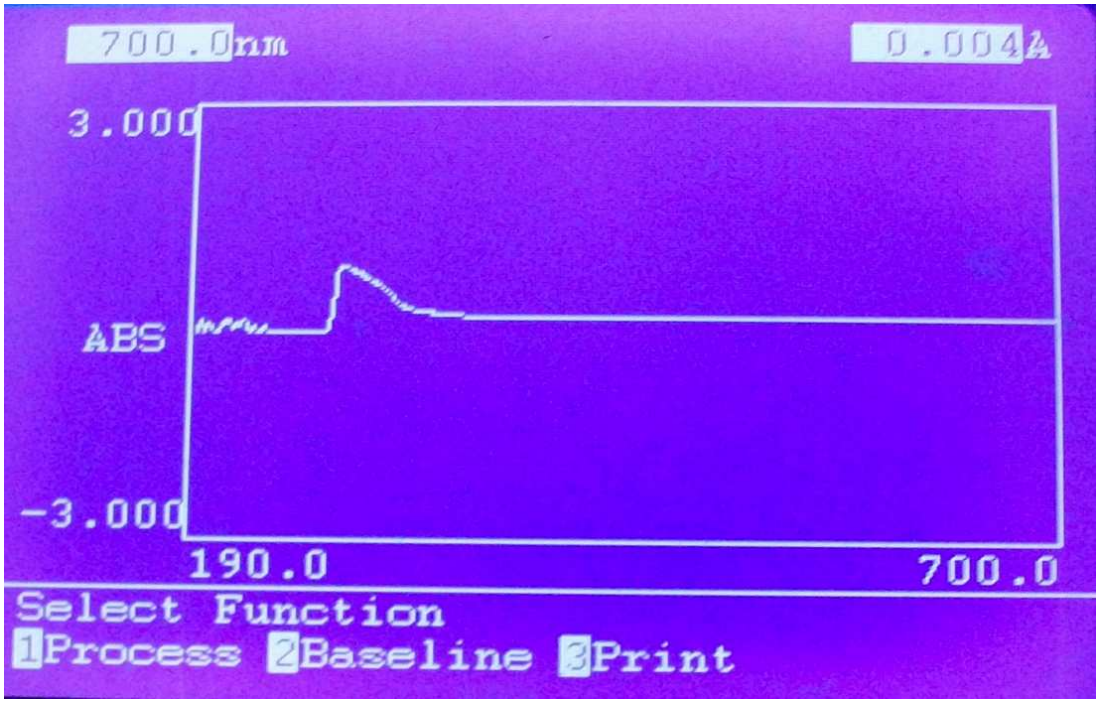

Figure E.2 Absorption of oil hexane mixture of the volume fraction A/4 between 190 nm and 700nm

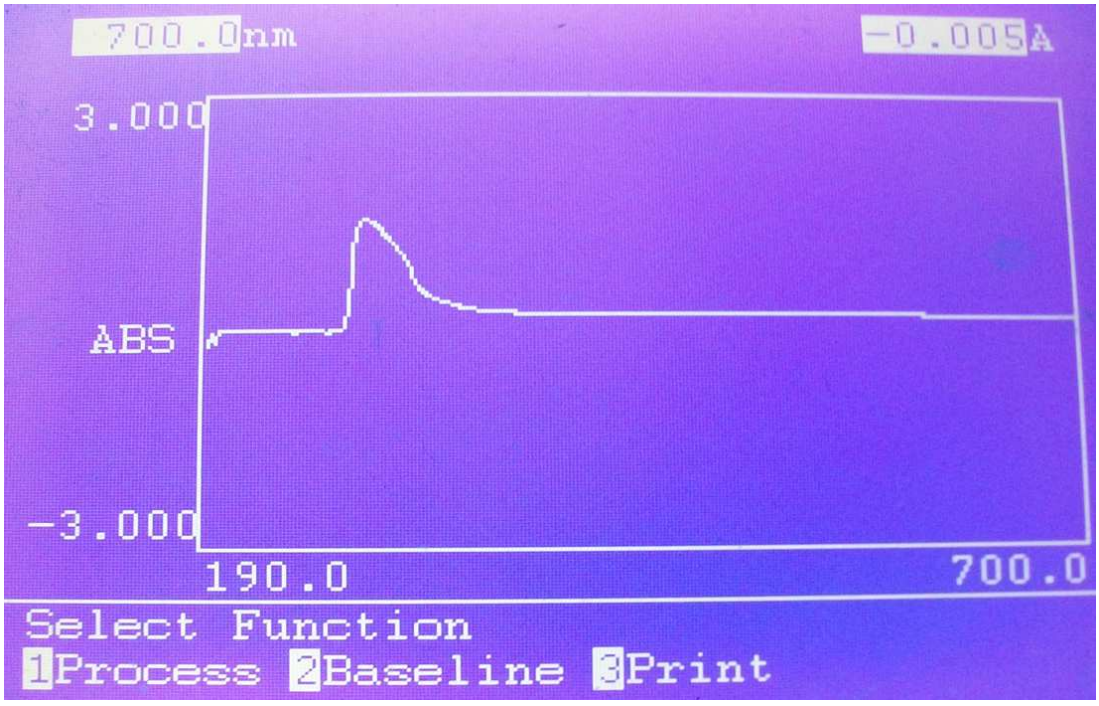

Figure E.3 Absorption of oil hexane mixture of the volume fraction A/2 between 190 nm and 700nm

E.3. Calibration Curves and Experimental Measuring Device's Specifications

In this part the calibration curves formed by the light absorption indexes of the oil-hexane mixtures with known volume concentrations are given. The formation of the curves repeated for three times and the average of three curves was used for calculating the volume concentration of the oil-hexane mixture retrieved by sampling tubes.

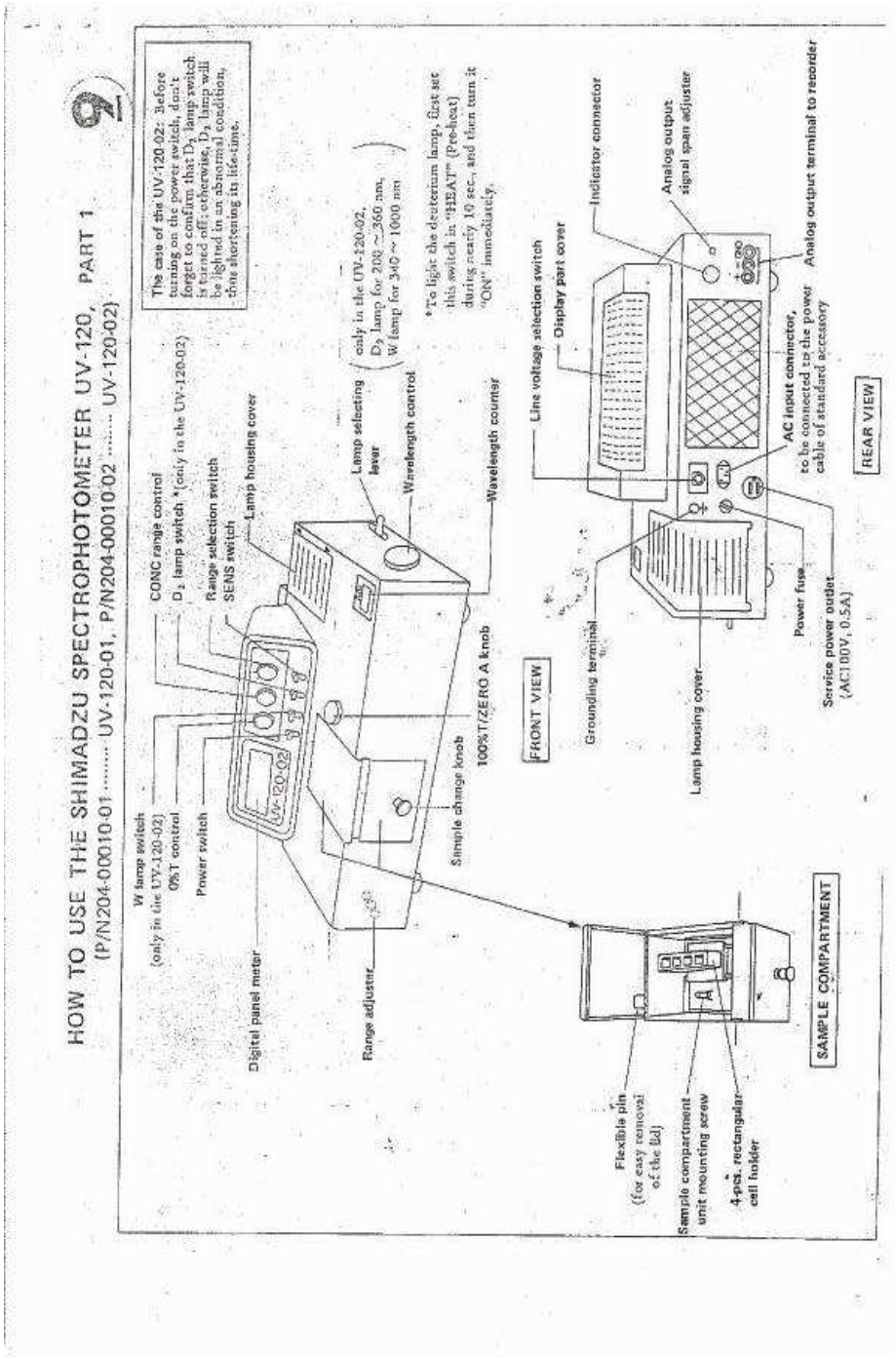

Figure E. 4 View of the Figure E.4 Shimadzu UV Spectrophotometer

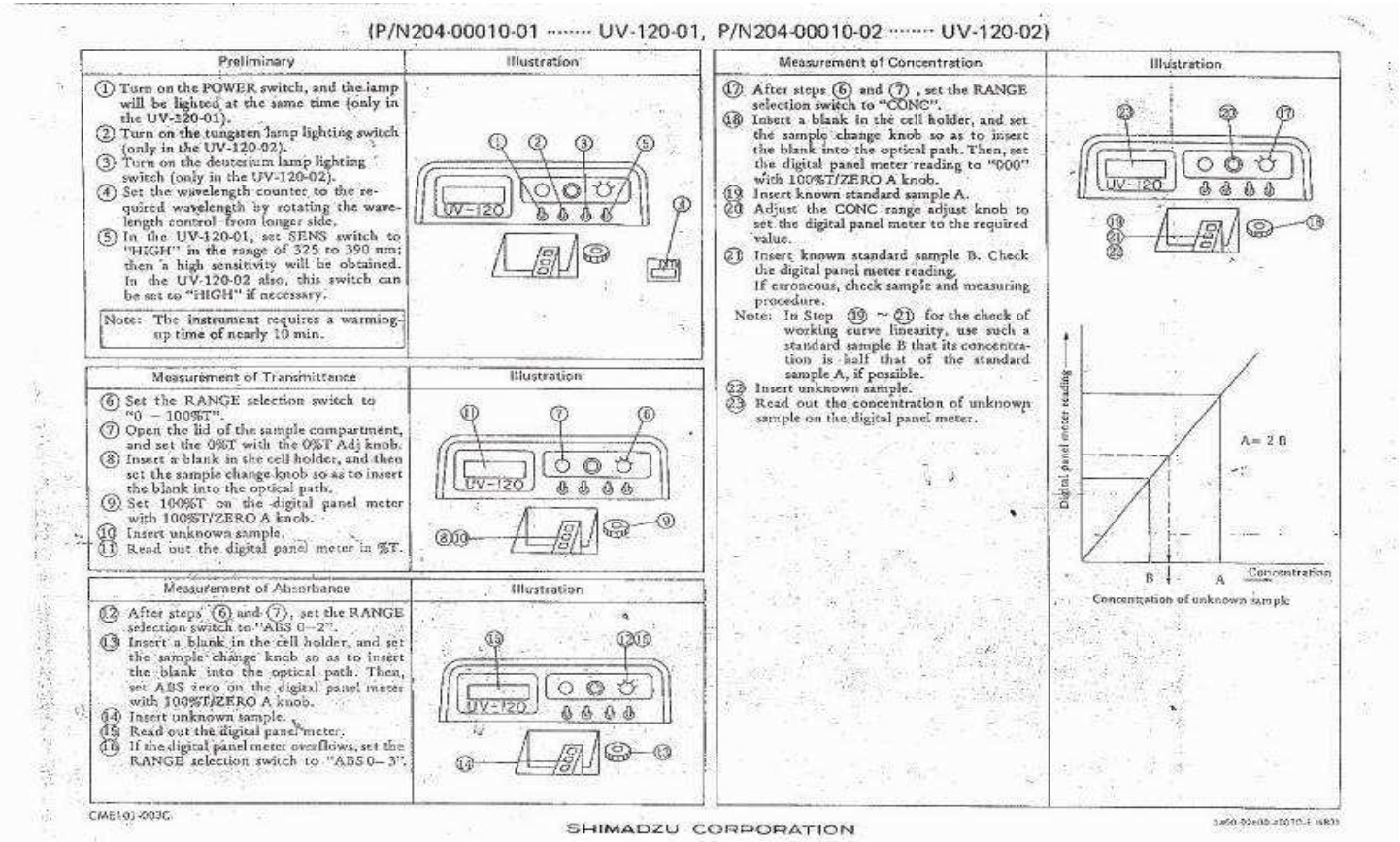

Figure E. 6 General usage of the Shimadzu UV Spectrophotometer